Journal of Statistical Physics, Vol. 81, Nos. 5/6, 1995

Fick's Law and Fractality of Nonequilibrium Stationary States in a Reversible Multibaker Map

Shuichi Tasaki[1] **and Pierre Gaspard**[2]

Received February 3, 1995; final April 18, 1995

Nonequilibrium stationary states are studied for a multibaker map, a simple reversible chaotic dynamical system. The probabilistic description is extended by representing a dynamical state in terms of a measure instead of a density function. The equation of motion for the cumulative function of this measure is derived and stationary solutions are constructed with the aid of deRham-type functional equations. To select the physical states, the time evolution of the distribution under a fixed boundary condition is investigated for an open multibaker chain of scattering type. This system corresponds to a diffusive flow experiment through a slab of material. For long times, any initial distribution approaches the stationary one obeying Fick's law. At stationarity, the intracell distribution is singular in the stable direction and expressed by the Takagi function, which is continuous but has no finite derivatives. The result suggests that singular measures play an important role in the dynamical description of nonequilibrium states.

KEY WORDS: Nonequilibrium states; Fick's law; fractal; singular measure; deRham equation; dynamical chaos.

1. INTRODUCTION

The understanding of transport properties is a long-standing problem in physics. Transport such as diffusion is described at the macroscopic level by phenomenological laws. In particular, Fick's law assumes that the flow of particles (**J**) is linearly proportional to the gradient of concentration

[1] Institute for Fundamental Chemistry, 34-4 Takano-Nishihiraki-cho, Sakyo-ku, Kyoto 606, Japan.

[2] Centre for Nonlinear Phenomena and Complex Systems, Université Libre de Bruxelles, Campus Plaine CP 231, 1050 Brussels, Belgium.

0022-4715/95/1200-0935$07.50/0

(∇C) in gases, liquids, or solids, the proportionality constant being minus the diffusion coefficient,

$$\mathbf{J} = -D\,\nabla C \tag{1.1}$$

Accordingly, if a difference of concentration is imposed at the boundaries of a slab of material, a linear concentration profile will establish itself by diffusion. In such a nonequilibrium stationary state, particles are diffusively migrating from one border to the other at a constant flow. Although this phenomenon has been described since the last century, how the microscopic reversible dynamics can accommodate such a nonequilibrium stationary state remains a mystery. The macroscopic aspects of Fick's law have been studied, in particular, in the framework of scaling statistical theories.[1] However, little is known on the microscopic aspects of these nonequilibrium diffusive states.

Recently, several works[2–9] have been devoted to the study of simple chaotic models of deterministic diffusion. In particular, a time-reversible area-preserving map[6–9]—referred to as a multibaker map—has been constructed as a spatially extended generalization of the baker map. This two-degree-of-freedom system of hyperbolic character shares with the Lorentz gas (with finite horizon) the property that diffusion is induced by dynamical instability. The Liouvillian dynamics, which rules the time evolution of nonequilibrium statistical ensembles, is exactly solvable for this piecewise-linear map. In this way, the Frobenius–Perron operator admits a generalized spectral decomposition in terms of the Pollicott–Ruelle resonances[10,11] and the associated eigendistributions, as shown elsewhere.[12] The relevance of the Pollicott–Ruelle resonances to the problem of diffusion comes from the fact that the spectrum of these resonances approaches the spectrum of the phenomenological diffusion equation in the limit of large wavenumbers of the diffusive eigenmodes.[6] In this regard, the Pollicott–Ruelle resonances and the associated eigendistributions provide us with the exact microscopic analogs of the eigenvalues and eigenfunctions of the macroscopic diffusion equation.[6] Beyond the invariant state which is uniform in space and corresponds to the microcanonical ensemble, the other eigendistributions correspond to decaying eigenmodes of diffusion.

The novelty of this approach is that the generalized spectral decomposition of the time evolution operator displays the decay and relaxation rates of irreversible processes at the level of the microscopic phase-space dynamics and without any modification of the laws of motion. The possibility and generality of such a relation between the time evolution operator and the characteristic time scales of irreversible phenomena have been emphasized and discussed over the last 30 years by Prigogine and

co-workers.[13,14] Thanks to the recent advances in dynamical system theory, a new and promising perspective is given to this possibility in the study of nonequilibrium statistical mechanics.

In the present paper, we exactly construct in a multibaker map the nonequilibrium stationary states corresponding to constant gradients of concentration with the aim of understanding the mechanism by which such stationary states can be maintained under an area-preserving dynamics.

The model we use here is a variant of the four-adic multibaker described in ref. 6. Rather than vertically stretching phase space cells by a factor four as in ref. 6, the present version of the multibaker acts by horizontal stretching by a factor two, as explained in Section 2. Accordingly, we refer to it as the dyadic multibaker. In Section 3, a general description of the time evolution of probability measures is introduced in terms of cumulative functions. In Section 4, solutions of the equation of motion corresponding to homogeneous stationary states are constructed with the aid of the deRham-type functional equations. *A priori*, the solutions possess intercell concentration profiles which are either linear or exponential. The intracell distribution is always singular along the stable direction, although the distribution along the unstable direction is smooth in the case of a linear intercell profile but singular in the case of an exponential intercell profile. For the particular case of a linear profile, the intracell distribution along the stable direction is described by the well-known Takagi function, which has self-similar properties reminiscent of fractal objects. Moreover, further stationary states are constructed with the aid of the time reversal operation. In Section 5, their flow properties are discussed and it is shown that the state with exponential intercell profile corresponds to a flow of ballistic type. On the other hand, the state with a linear profile corresponds to a flow of diffusion type, obeying either the Fick or anti-Fick law, where the distribution is smooth along the unstable or stable directions, respectively.

In Section 6, using a time-evolution argument in a scattering configuration of the multibaker map where the concentration is fixed at both ends of a chain, we show that the linear concentration profiles satisfying Fick's law are selected. It turns out that the nonequilibrium stationary states with linear concentration profiles, whether they obey Fick's law or not, maximize the Kolmogorov–Sinai (KS) entropy per unit time that we define for these invariant states and, moreover, they satisfy Pesin's equality,[15,16] i.e., the equality of the KS entropy to the sum of positive Lyapunov exponents. We remark here that the determination of physical measures has been extensively studied in ergodic theory, where the Kolmogorov measure or the Sinai–Ruelle–Bowen (SRB) measure have been shown to be physically realizable in closed systems whether the

dynamics is uniformly or nonuniformly hyperbolic.[15,16] However, the present situation differs in several respects from the ones previously considered. In particular, the present system has an infinite spatial extension typical of open systems of nonequilibrium statistical mechanics, in contrast with the closed and finite systems. Accordingly, new types of invariant measures corresponding to nonequilibrium stationary states become possible, which have not yet been described in the literature. This point is further discussed in Sections 4, 5, and 8. In Section 7, the escape-time distribution is discussed and is shown to be related to the derivative of Takagi-type functions. This result shows the deep relation existing between the nonequilibrium stationary states and the phenomenon of chaotic scattering.[6,7] Section 8 is devoted to concluding remarks, in particular, about the relation of the physical nonequilibrium stationary states to the eigendistributions constructed elsewhere.[7,12]

The present study reveals the role of singular measures with self-similar fractal-like properties in nonequilibrium stationary states. We conjecture that these properties are general and also arise in other deterministic systems sustaining nonequilibrium stationary states compatible with Fick's law. Preliminary results of the present study were reported at the 7th Toyota Conference.[17]

2. MULTIBAKER MAP

The multibaker map is an area-preserving map which is defined on a periodic array of countably many unit squares and which exhibits diffusion processes. A 4-adic multibaker map has been proposed by one of us[6] and the properties of diffusion and nonequilibrium states have been rigorously studied with the aid of zeta functions and of the "thermodynamic formalism." Multibaker maps admit the Lebesgue measure as an invariant measure and the deviations from this equilibrium state decay via diffusion processes. The decay properties of the deviations are described by the corresponding Frobenius–Perron operator. The spectral properties of the Frobenius–Perron operator have been recently studied by Gaspard,[7] Hasegawa and Driebe,[8] and Tasaki *et al.*[9] Thanks to the periodicity of the system, the Fourier transform of the Frobenius–Perron operator is block diagonal with respect to the quasimomentum. Each Fourier component of the Frobenius–Perron operator acquires a Jordan block structure once it is extended to a larger functional space than the Hilbert space of square integrable functions. The logarithms of the eigenvalues of the Frobenius–Perron operator give the decay rates of the correlation functions,[7–9] which are known as Pollicott–Ruelle resonances.[10,11,16]

In this paper, we study the properties of nonequilibrium stationary states for the simplest multibaker map defined on a one-dimensional array of unit squares:

$$B(n, x, y) = \begin{cases} \left(n-1, 2x, \dfrac{y}{2}\right), & 0 \leqslant x < \dfrac{1}{2} \\ \left(n+1, 2x-1, \dfrac{y+1}{2}\right), & \dfrac{1}{2} \leqslant x < 1 \end{cases} \tag{2.1}$$

where an integer n labels the unit squares and a pair (x, y) of real numbers $(0 \leqslant x < 1,\ 0 \leqslant y < 1)$ stands for the coordinates in each unit square. The map B is schematically depicted in Fig. 1. This map is area preserving, so that it admits the Liouville measure, $dx\,dy$, as an invariant measure.

The map B is invertible with the following inverse:

$$B^{-1}(n, x, y) = \begin{cases} \left(n+1, \dfrac{x}{2}, 2y\right), & 0 \leqslant y < \dfrac{1}{2} \\ \left(n-1, \dfrac{x+1}{2}, 2y-1\right), & \dfrac{1}{2} \leqslant y < 1 \end{cases} \tag{2.2}$$

Moreover, the system is time-reversal invariant, i.e., there exists an involution I satisfying

$$B^{-1} = IBI \tag{2.3}$$

which corresponds to the velocity inversion in the particle system

$$I(n, x, y) \equiv (n, 1-y, 1-x) \tag{2.4}$$

The multibaker map B is uniformly hyperbolic with a stretching factor 2 and thus possesses a positive Lyapunov exponent equal to ln 2.

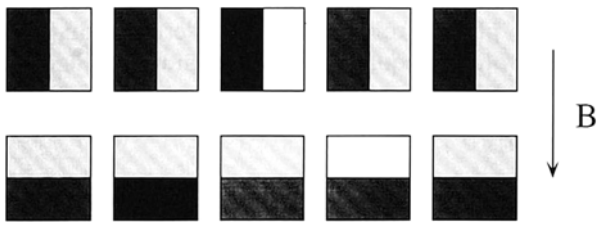

Fig. 1. Action of the multibaker map B defined by Eq. (2.1) on its phase space composed of an infinite chain of squares.

3. DYNAMICAL STATES AND THEIR TIME EVOLUTION

In the conventional probabilistic description, the so-called Liouvillian description (e.g., refs. 13 and 18), dynamical states are specified by smooth density functions. The density functions univocally determine corresponding measures which are absolutely continuous with respect to the Liouville measure and conversely. If the measure is not absolutely continuous with respect to the Liouville measure, the previous description must be extended by representing the dynamical state *directly* in terms of the cumulative function which is the integral of the density when this latter exists. The following developments are based on this approach in terms of cumulative functions rather than on densities.

On this ground, we consider the time evolution of a measure μ describing a dynamical state under the multibaker map. We assume that the measure is a Borel measure. Under this condition, any μ-measurable set is expressed as a countable union of semiopen rectangles:

$$\{[0, x) \times [0, y)\}_n \tag{3.1}$$

where the subscript n indicates that the rectangle $[0, x) \times [0, y)$ is a subset of the nth unit square. As a result, the measure μ is completely specified by the cumulative function G:

$$G(n, x, y) \equiv \mu(\{[0, x) \times [0, y)\}_n) \tag{3.2}$$

In similarity with the proof of Liouville's theorem (e.g., ref. 18); the time evolution of the measure is found to be

$$\mu_{t+1}(A) = \mu_t(B^{-1}A) \tag{3.3}$$

where μ_t stands for the measure at time t and A is an arbitrary measurable set. Equation (3.3) plays a role of the Liouville equation. Equation (3.3) induces the time-evolution equation for the cumulative function G. Since

$$B^{-1}\{[0, x) \times [0, y)\}_n$$

$$= \begin{cases} \{[0, x/2) \times [0, 2y)\}_{n+1}, & 0 \leqslant y < \frac{1}{2} \\ \{[0, x/2) \times [0, 1)\}_{n+1} & \\ \quad \cup \{[1/2, (x+1)/2) \times [0, 2y-1)\}_{n-1}, & \frac{1}{2} \leqslant y < 1 \end{cases} \tag{3.4}$$

we obtain

$$G_{t+1}(n, x, y) = \begin{cases} G_t\left(n+1, \frac{x}{2}, 2y\right), & 0 \leqslant y < \frac{1}{2} \\ G_t\left(n+1, \frac{x}{2}, 1\right) + G_t\left(n-1, \frac{x+1}{2}, 2y-1\right) & \\ \quad - G_t\left(n-1, \frac{1}{2}, 2y-1\right), & \frac{1}{2} \leqslant y \leqslant 1 \end{cases} \tag{3.5}$$

where $G_t(n, x, y) = \mu_t(\{[0, x) \times [0, y)\}_n)$ is the cumulative function of the measure at time t.

Setting $x = 1$ and $y = 1$ in (3.5), we have

$$\begin{aligned} G_{t+1}(n, 1, 1) &= G_t(n+1, \tfrac{1}{2}, 1) + G_t(n-1, 1, 1) - G_t(n-1, \tfrac{1}{2}, 1) \\ &= \alpha_{n+1,t} G_t(n+1, 1, 1) + (1 - \alpha_{n-1,t}) G_t(n-1, 1, 1) \end{aligned} \tag{3.6a}$$

with

$$\alpha_{n,t} \equiv \frac{G_t(n, 1/2, 1)}{G_t(n, 1, 1)} \tag{3.6b}$$

Since $G_t(n, 1, 1)$ is nonnegative and $G_t(n, 1/2, 1) \leqslant G_t(n, 1, 1)$, $\alpha_{n,t}$ satisfies $0 \leqslant \alpha_{n,t} \leqslant 1$. Therefore, Eq. (3.6a) represents a random walk with $\alpha_{n,t}$ being the transition probability from left to right at site n and time t. As $\alpha_{n,t}$ can take any real values, (3.6a) implies that the multibaker map contains uncountably many random walks.

4. HOMOGENEOUS STATIONARY STATES AND DERHAM-TYPE EQUATION

4.1. Solving the Equation by Separation

We now turn our attention to stationary states, which correspond to invariant measures and thus to time-independent solutions of (3.5):

$$G(n, x, y) = \begin{cases} G\left(n+1, \frac{x}{2}, 2y\right), & 0 \leqslant y < \frac{1}{2} \\ G\left(n+1, \frac{x}{2}, 1\right) + G\left(n-1, \frac{x+1}{2}, 2y-1\right) & \\ \quad - G\left(n-1, \frac{1}{2}, 2y-1\right), & \frac{1}{2} \leqslant y \leqslant 1 \end{cases} \tag{4.1}$$

Since the x and y directions are mapped onto themselves in the multibaker map and are therefore independent, we can expect the existence of a product invariant measure, for which the cumulative function is a product of functions of x and y:

$$G(n, x, y) = G(n, 1, y)\, F(n, x) \tag{4.2}$$

The functions $G(n, 1, y)$ and $F(n, x)$ represent the distribution along the stable y direction and the unstable x direction respectively.

It turns out that the functional equation (4.1) is a separable equation in the sense that it can be separated into two distinct equations respectively for $G(n, 1, y)$ and for $F(n, x)$. In order to achieve this separation, we introduce a separation constant α which is taken to be $\alpha = F(n, 1/2)$. To guarantee the positivity of the measure, we have the condition that $0 < \alpha < 1$.

By substituting $x = 1$ into (4.1) and using (4.2), we obtain an equation for $G(n, 1, y)$:

$$G(n, 1, y) = \begin{cases} \alpha G(n+1, 1, 2y), & 0 \leqslant y < \frac{1}{2} \\ (1-\alpha)\, G(n-1, 1, 2y-1) + \alpha G(n+1, 1, 1), & \frac{1}{2} \leqslant y \leqslant 1 \end{cases} \tag{4.3}$$

Note that, for $y = 1$, (4.3) reduces to a recursion relation for $G(n, 1, 1)$:

$$G(n, 1, 1) = (1-\alpha)\, G(n-1, 1, 1) + \alpha G(n+1, 1, 1) \tag{4.4}$$

which admits a solution depending on two parameters to be fixed by boundary conditions.

The equation corresponding to F can also be derived from Eqs. (4.1)–(4.3):

$$F(n, x) = \begin{cases} \alpha F(n-1, 2x), & 0 \leqslant x < \frac{1}{2} \\ (1-\alpha)\, F(n+1, 2x-1) + \alpha, & \frac{1}{2} \leqslant x \leqslant 1 \end{cases} \tag{4.5}$$

For instance, the first relation of (4.5) is deduced from the first relation of (4.1) by using the condition for the product measure (4.2) and Eq. (4.3) for $G(n, 1, y)$, for $y < 1/2$,

$$\begin{aligned} G(n, x, y) &= G(n, 1, y)\, F(n, x) \\ &= \alpha G(n+1, 1, 2y)\, F(n, x) \\ &= G(n+1, x/2, 2y) \\ &= G(n+1, 1, 2y)\, F(n+1, x/2) \end{aligned}$$

Replacing n by $n-1$ and x by $2x$, the first relation of (4.5), $F(n, x) = \alpha F(n-1, 2x)$, follows.

The functional equations (4.3) and (4.5) are similar to the deRham equation.[19–22] These equations play a central role in this paper, where our goal is to perform their resolution.

4.2. Equation for the Unstable *x* Direction

Equation (4.5) admits a unique continuous solution. Indeed, it is a fixed-point equation of the transformation $\mathscr{T}_1$ defined by

$$\mathscr{T}_1 f(n, x) \equiv \begin{cases} \alpha f(n+1, 2x), & 0 \leqslant x < \frac{1}{2} \\ (1-\alpha) f(n-1, 2x-1) + \alpha, & \frac{1}{2} \leqslant x \leqslant 1 \end{cases} \tag{4.6}$$

Since

$$\| \mathscr{T}_1 f - \mathscr{T}_1 g \| \equiv \sup_{\substack{n \in \mathbf{N}, \, 0 \leqslant x \leqslant 1 \\ 0 \leqslant y \leqslant 1}} |\mathscr{T}_1 f(n, x) - \mathscr{T}_1 g(n, x)| \leqslant \bar{\alpha} \, \| f - g \| \tag{4.7}$$

with $\bar{\alpha} = \max\{\alpha, 1-\alpha\} < 1$, the transformation is contractive and, as a result, its fixed point exists and is unique. Moreover, the transformation $\mathscr{T}_1$ keeps the continuity for functions such that $f(n, 1) \equiv 1$, i.e., the continuity of f and the condition $f(n, 1) \equiv 1$ implies the continuity of $\mathscr{T}_1 f$. Accordingly, the fixed point of $\mathscr{T}_1$ can be uniformly approximated by a sequence of continuous functions and is also continuous.

Equation (4.5) does not depend explicitly on the cell index n, so that the cumulative function along the unstable direction $F(n, x)$ is given by

$$F(n, x) = f_\alpha(x) \tag{4.8}$$

where the function f_α is defined as the solution of the deRham equation[19]

$$f_\alpha(x) = \begin{cases} \alpha f_\alpha(2x), & 0 \leqslant x < \frac{1}{2} \\ (1-\alpha) f_\alpha(2x-1) + \alpha, & \frac{1}{2} \leqslant x \leqslant 1 \end{cases} \tag{4.9}$$

Such solutions correspond to a measure which can be referred to as homogeneous stationary states. In contrast, there also exist stationary states which are not homogeneous if separation constants α_n are used which depend on the cell index n. We do not consider here these inhomogeneous stationary states.

As studied in refs. 19 and 20, the solution of (4.9) for $\alpha \neq 1/2$ is a Lebesgue singular function, i.e., a monotonically increasing continuous function with zero derivatives almost everywhere but nondifferentiable on a dense set of points. About the properties of the function f_α, see also

refs. 23 and 24. However, in the limit $\alpha = 1/2$, the solution becomes $f_{1/2}(x) = x$, which is differentiable. In this case, the distribution is uniform along the unstable x direction.

4.3. Equation Along the Stable y Direction

We now turn to the other functional equation (4.3), which concerns the cumulative function $G(n, 1, y)$ along the stable y direction. This equation is similar to Eq. (4.5) except that it admits a unique continuous solution for several possible values of the sequence $\{G(n, 1, 1)\}$. According to the value of the parameter α, two cases should be distinguished:

(a) $\alpha \neq 1/2$, $0 < \alpha < 1$. In this case, Eq. (4.4) gives

$$G(n, 1, 1) = A_1 \left(\frac{1-\alpha}{\alpha} \right)^n + A_2 \tag{4.10}$$

where A_1 and A_2 are constants to be determined by the boundary conditions. By substituting (4.10) into (4.3) and by assuming that $G(n, 1, y)$ depends on the cell coordinate n in the same way as (4.10), we obain the cumulative function along the y direction

$$G(n, 1, y) = A_1 \left(\frac{1-\alpha}{\alpha} \right)^n f_{1-\alpha}(y) + A_2 f_\alpha(y)$$

The cumulative function over the whole phase space is thus given by

$$G(n, x, y) = f_\alpha(x)\, G(n, 1, y) = f_\alpha(x) \left[A_1 \left(\frac{1-\alpha}{\alpha} \right)^n f_{1-\alpha}(y) + A_2 f_\alpha(y) \right] \tag{4.11}$$

The intercell distribution is exponential with respect to the cell coordinate [cf. Eq. (4.10)], while the intracell distribution is singular since it is expressed by the Lebesgue singular function f_α. The inter- and intracell distributions are depicted in Figs. 2a and 2b–2c, respectively.

(b) $\alpha = 1/2$. In this case, Eq. (4.4) gives

$$G(n, 1, 1) = nB_1 + B_2 \tag{4.12}$$

where B_1 and B_2 are constants to be fixed here also by the boundary conditions. In similarity with the resolution of the previous case, we substitute Eq. (4.12) into (4.3) and, by assuming that $G(n, 1, y)$ depends on the cell coordinate n in the same way as (4.12), we finally obtain the cumulative function over the whole phase space as

$$G(n, x, y) = xG(n, 1, y) = x\{B_1[ny + T(y)] + B_2 y\} \tag{4.13}$$

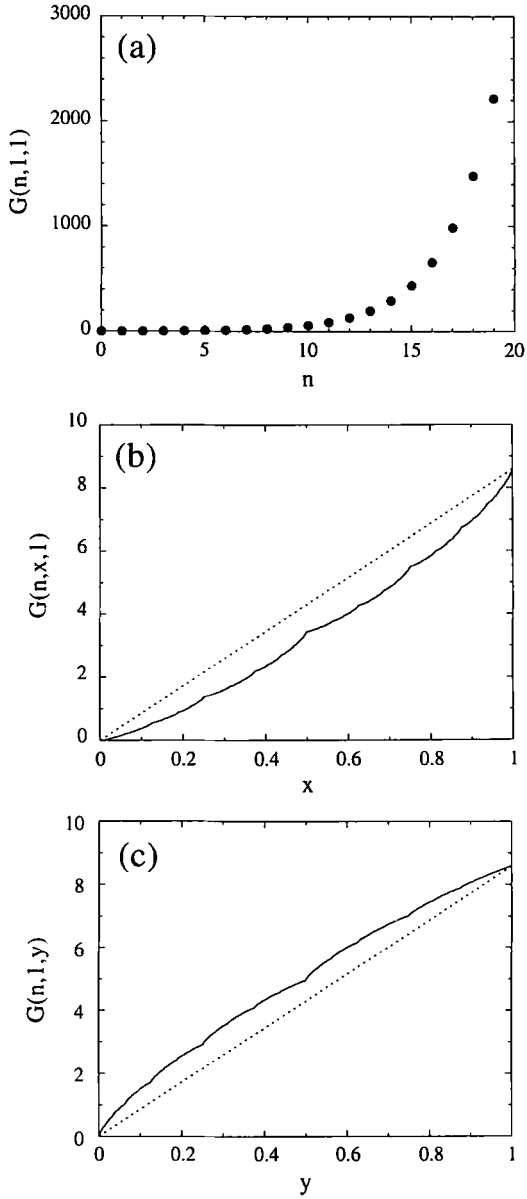

Fig. 2. For $\alpha = 2/5 \neq 1/2$, cumulative function (4.11) of a non-Fickian nonequilibrium stationary state: (a) intercell distribution given by $G(n, 1, 1) = (3/2)^n + 1$; (b) intracell distribution along the x axis (unstable direction) given by $G(n, x, 1) = [(3/2)^n + 1] f_{2/5}(x)$ with $n = 5$; (c) intracell distribution along the y axis (stable direction) given by $G(n, 1, y) = (3/2)^n f_{3/5}(y) + f_{2/5}(y)$ with $n = 5$.

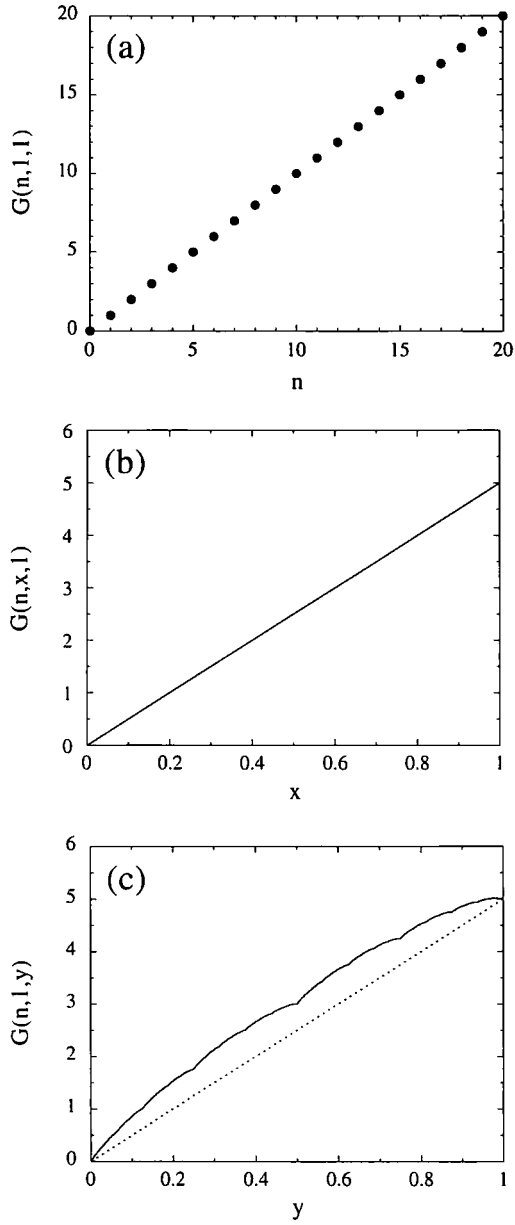

Fig. 3. For $\alpha = 1/2$, cumulative function (4.13) of a Fickian nonequilibrium stationary state: (a) intercell distribution given by $G(n, 1, 1) = n$; (b) intracell distribution along the x axis (unstable direction) given by $G(n, x, 1) = nx$ with $n = 5$; (c) intracell distribution along the y axis (stable direction) given by $G(n, 1, y) = ny + T(y)$ with $n = 5$.

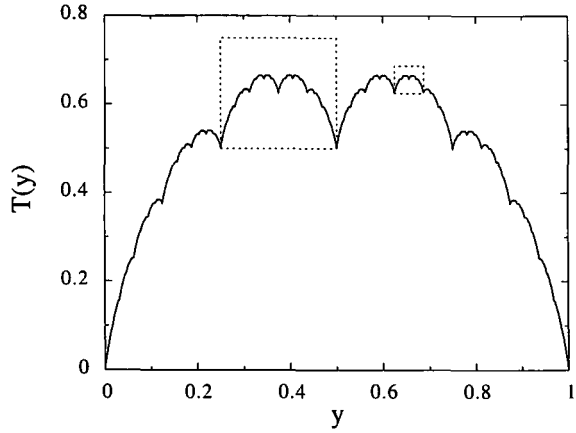

Fig. 4. The Takagi function $T(y)$ and some of its self-similar parts.

where $T(y)$ obeys the following functional equation:

$$T(y) = \begin{cases} \frac{1}{2}T(2y) + y, & 0 \leqslant y < \frac{1}{2} \\ \frac{1}{2}T(2y-1) + 1 - y, & \frac{1}{2} \leqslant y \leqslant 1 \end{cases} \tag{4.14}$$

We remark that the intercell distribution here is linear with respect to the cell coordinates [cf. (4.12)]. On the other hand, the intracell distribution is also linear along the unstable x direction, but it is singular in the stable y direction. The inter- and intracell distributions are depicted in Figs. 3a and 3b–3c, respectively. The singularity of the distribution is due to the function $T(y)$, which was first introduced by Takagi[25] as a pathological example of a continuous function without finite derivatives everywhere and which is known as the Takagi function. The Takagi function is shown in Fig. 4. The function presents a self-similarity: The parts enclosed by rectangles are similar to the whole function. This self-similarity is at the very origin of its singularity. The properties of the Takagi function and of related functions have been extensively investigated by Hata and Yamaguti.[20,21]

4.4. The Effect of Time Reversal

After the previous construction of the homogeneous stationary states, we discuss the consequences of time-reversal symmetry. Since the multibaker map B is symmetric under time reversal, the time-reversal operation transforms stationary states into other stationary states. Accordingly, we get the following results.

(c) Time Reversal of $\alpha \neq 1/2$, $0 < \alpha < 1$. The cumulative function $\bar{G}_\alpha(n, x, y)$ of the time-reversed state is given by

$$\begin{aligned}
\bar{G}_\alpha(n, x, y) &\equiv \mu(I\{[0, x) \times [0, y)\}_n) \\
&= \mu(\{(1-y, 1] \times (1-x, 1]\}_n) \\
&= G(n, 1, 1) + G(n, 1-y, 1-x) \\
&\quad - G(n, 1-y, 1) - G(n, 1, 1-x) \\
&= [1 - f_\alpha(1-y)] \left\{ A_1 \left(\frac{1-\alpha}{\alpha} \right)^n [1 - f_{1-\alpha}(1-x)] \right. \\
&\quad \left. + A_2 [1 - f_\alpha(1-x)] \right\} \\
&= f_{1-\alpha}(y) \left[A_1 \left(\frac{1-\alpha}{\alpha} \right)^n f_\alpha(x) + A_2 f_{1-\alpha}(x) \right] \qquad (4.15)
\end{aligned}$$

where we have used the following relation, which is easily derived from the deRham equation (4.9):

$$f_\alpha(1-x) + f_{1-\alpha}(x) = 1 \qquad (4.16)$$

The intercell distribution of the reversed state (4.15) is identical with the original one. Indeed, comparing (4.15) with (4.11), one finds that the n-dependent part is invariant under the time-reversal operation. Moreover, the n-independent part belongs to the same class as the original one, since they are related by the parameter change $\alpha \leftrightarrow 1-\alpha$. Therefore, the time-reversal operation does not produce stationary states of a new type in this case.

(d) Time Reversal of $\alpha = 1/2$. Because of the property $T(1-x) = T(x)$, the cumulative function $\bar{G}_{1/2}(n, x, y)$ of the time-reversed state is given by

$$\bar{G}_{1/2}(n, x, y) = y\{B_1[nx - T(x)] + B_2 x\} \qquad (4.17)$$

for which the intercell distribution is here also identical with the original one. However, the original distribution (4.13) is regular in the unstable x direction and singular in the stable y direction, although the time-reversed state (4.17) is singular in the unstable x direction and regular in the stable y direction. Therefore, Eq. (4.17) defines a new stationary state.

4.5. Symbolic Dynamics, Markov Chain, and the KS Entropy

Here, we establish a symbolic dynamics for the multibaker and the isomorphism with a Markov chain, which allows us to calculate the KS entropy of the stationary states. The multibaker map B together with a measure μ_α determined by Eqs. (4.3) and (4.5) is isomorphic to a probabilistic Markov chain in the sense of Ornstein.[26] The isomorphism is induced from the following symbolic representation. A bilateral sequence $\omega = \{\omega_n\}_{-\infty < n < +\infty}$ of integers ω_n is associated to each point $p \equiv (n, x, y)$ of the phase space in such a way that $\omega_n = k$ if and only if $B^n p$ belongs to the kth unit square. In this symbolic representation, the map B acts as a left shift. The measure μ_α naturally induces a shift-invariant Markov measure μ_α^S on the space of symbolic sequences. Indeed, the measure of a cylindrical set corresponding to a finite sequence $\bar{\omega} \equiv (\omega_{-M}, \omega_{-M+1}, \ldots, \omega_N)$ of length $N+M+1$ is given by

$$\begin{aligned}\mu_\alpha^S(\bar{\omega}) &= \mu_\alpha^S(\omega_{-M}, \omega_{-M+1}, \ldots, \omega_N) \\ &= G(\omega_{-M}, 1, 1)\, P_{\omega_{-M}\omega_{-M+1}} P_{\omega_{-M+1}\omega_{-M+2}} \cdots P_{\omega_{N-1}\omega_N}\end{aligned} \tag{4.18}$$

where $G(\omega_{-M}, 1, 1)$ is the measure of the ω_{-M}th unit square and the transition probability P_{ij} is defined as

$$P_{ij} = \begin{cases} \alpha, & i = j+1 \\ 1-\alpha, & i = j-1 \\ 0, & \text{otherwise} \end{cases} \tag{4.19}$$

Details of the proof are given in Appendix A. Its KS entropy $h_{KS}(B, \mu_\alpha)$ is then given by (e.g., ref. 27; see also ref. 6)

$$\begin{aligned}h_{KS}(B, \mu_\alpha) &= \lim_{N, M \to +\infty} \frac{-\sum_{i=-N}^{M} \sum_j G(i, 1, 1)\, P_{ij} \ln P_{ij}}{\sum_{i=-N}^{M} G(i, 1, 1)} \\ &= -[\alpha \ln \alpha + (1-\alpha) \ln(1-\alpha)]\end{aligned} \tag{4.20}$$

where the denominator $\sum_{i=-N}^{M} G(i, 1, 1)$ is introduced in order to normalize the measure $G(i, 1, 1)$.

The entropy of the time-reversed state $\bar{\mu}_\alpha$ is calculated in two steps. First, the inverse transformation B^{-1} with the time-reversed state $\bar{\mu}_\alpha$ is isomorphic to the multibaker map B with the original state μ_α via the time-reversal operation I: $B^{-1} = IBI$, $\bar{\mu}_\alpha = I\mu_\alpha$. Thus, their entropies are the same[27]: $h_{KS}(B^{-1}, \bar{\mu}_\alpha) = h_{KS}(B, \mu_\alpha)$. Moreover, since the entropy of the

map B^{-t} is proportional to the absolute value of t,[27] $h_{KS}(B^{-t}, \bar{\mu}_\alpha) = |t|\, h_{KS}(B^{-1}, \bar{\mu}_\alpha)$, we have

$$\begin{aligned} h_{KS}(B, \bar{\mu}_\alpha) &= |-1|\, h_{KS}(B^{-1}, \bar{\mu}_\alpha) \\ &= h_{KS}(B, \mu_\alpha) \\ &= -[\alpha \ln \alpha + (1-\alpha)\ln(1-\alpha)] \end{aligned} \tag{4.21}$$

On the other hand, the Lyapunov exponent of the multibaker map B is equal to $\lambda = \ln 2$. The equality between the KS entropy and the Lyapunov exponent, i.e., Pesin's equality, is therefore obtained only when $\alpha = 1/2$, where the KS entropy (4.21) reaches its maximum. However, we remark that the invariant measures we construct are all different from the equilibrium invariant measure, which is the Lebesgue measure $G_{eq}(n, x, y) = xy$. One of the main differences lies in the singular character of the measures μ_α. Before closing this section, we comment on an important implication of this aspect.

Since the cumulative function is composed of singular functions such as f_α and the Takagi function (except in the case where $\alpha = 1/2$ and $B_1 = 0$), the corresponding invariant measures are not absolutely continuous with respect to the Lebesgue measure. As a consequence, they cannot be expressed in terms of density functions $\rho(n, x, y)$:

$$G(n, x, y) \neq \int_0^x dx' \int_0^y dy'\, \rho(n, x', y') \tag{4.22}$$

Therefore, it was essential to consider the time evolution of the measure directly represented by its cumulative function rather than by its density function, in contrast with conventional treatments of statistical mechanics. According to Mandelbrot, self-similar and singular functions like the Takagi function are referred to as fractals. In this respect, an important implication of our results is that nonequilibrium stationary states of mechanical systems have to be described in terms of singular measures. Indeed, the above rigorous construction of nonequilibrium stationary states for the multibaker provides a counterexample to the current assumption that nonequilibrium stationary states can be described by density functions. This assumption is known to hold for stochastic descriptions of nonequilibrium phenomena based on a kinetic equation like the Fokker–Planck equation. However, the above result shows that this assumption cannot hold in general and, in particular, at the microscopic level of the Liouvillian dynamics.

5. FLOW IN STATIONARY STATES, FICK LAW, AND ANTI-FICK LAW

We consider the flow of the uniform stationary states obtained in the previous section. The flow of particles across the boundary between the nth and $(n+1)$th unit squares can be defined in the following way. Under the multibaker map B, the half-square $[1/2, 1)\times[0, 1)$ in the nth unit square moves to the right and the half-square $[0, 1/2)\times[0, 1)$ in the $(n+1)$th unit square moves to the left. Thus, the flow $J_{n|n+1}$ from left to right at the n–$(n+1)$ boundary is given by (cf. Fig. 5)

$$\begin{aligned} J_{n|n+1} &= \mu(\{[\tfrac{1}{2}, 1)\times[0, 1)\}_n) - \mu(\{[0, \tfrac{1}{2})\times[0, 1)\}_{n+1}) \\ &= G(n, 1, 1) - G(n, \tfrac{1}{2}, 1) - G(n+1, \tfrac{1}{2}, 1) \end{aligned} \tag{5.1}$$

We apply this formula to the three cases which have been previously distinguished.

(a) $\alpha \neq 1/2$, $0 < \alpha < 1$. The flow corresponding to Eq. (4.10) is therefore

$$J_{n|n+1} = (1-\alpha)\, G(n, 1, 1) - \alpha G(n+1, 1, 1) = (1-2\alpha)\, A_2 \tag{5.2}$$

In this case, the flow is due to the term of (4.10) which is independent of the cell coordinate n. This part of the measure gives a weight αA_2 to the left-hand half of each cell and a weight $(1-\alpha)\, A_2$ to the right-hand half. One iteration of the multibaker map induces a left-to-right flow of $(1-\alpha)\, A_2$ and a right-to-left flow of αA_2, and as a result, a net flow of $(1-2\alpha)\, A_2$ from left to right. In other words, the difference of the weights of the half-cells is at the origin of the flow. In this sense, the flow (5.2) corresponds to a ballistic motion. On the contrary, the term of (4.10) which depends on the cell coordinate n does not contribute to the net flow.

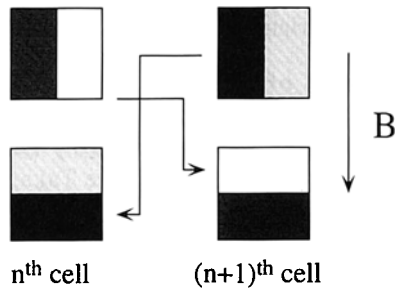

Fig. 5. The flow $J_{n|n+1}$ induced by the multibaker and given by Eq. (5.1).

This can be regarded as a consequence of the cancellation between the ballistic and diffusive flows. Indeed, Eq. (5.2) can be rewritten as

$$J_{n|n+1} = (1-2\alpha)\frac{G(n,1,1)+G(n+1,1,1)}{2}$$

$$-\frac{1}{2}[G(n+1,1,1)-G(n,1,1)] \tag{5.3}$$

which is a sum of the ballistic flow (the first term) and of the diffusive flow (the second term). These two flows cancel each other for the n-dependent term of (4.10). On the other hand, the n-independent term of (4.10) generates only the ballistic flow, but not the diffusive flow.

(b) $\alpha = 1/2$. On the other hand, the distribution (4.12) gives the flow

$$J_{n|n+1} = -\frac{B_1}{2} = -\frac{1}{2}[G(n+1,1,1)-G(n,1,1)] \tag{5.4}$$

Contrary to the previous case, the flow is here due to the nonuniformity of the distribution, i.e., to the term of (4.12) which depends on the cell coordinate n. The flow is here proportional to the gradient $G(n+1,1,1)-G(n,1,1)$ with a negative constant $-1/2$. By the same arguments as in refs. 6–9, one can easily see that this constant gives the diffusion coefficient $D=1/2$ of the multibaker map B. Therefore, the relation (5.4) is nothing but Fick's law:

$$J_{n|n+1} = -D[G(n+1,1,1)-G(n,1,1)] \tag{5.5}$$

so that diffusion is at the origin of the flow.

(c) Time Reversal of $\alpha = 1/2$. Although the intercell distribution of the time-reversed state (4.17) is the same as for the original state (4.13) [i.e., is equal to (4.12)], the flow given by (5.1) is different for the time-reversed state because of the term with the Takagi function, so that an anti-Fick law appears:

$$\bar{J}_{n|n+1} = \tfrac{1}{2}B_1 = \tfrac{1}{2}[\bar{G}_{1/2}(n+1,1,1)-\bar{G}_{1/2}(n,1,1)]$$

$$= D[\bar{G}_{1/2}(n+1,1,1)-\bar{G}_{1/2}(n,1,1)] \tag{5.6}$$

where the flow is positively proportional to the concentration difference. It is important to note the role of the intracell distribution in the derivation of this result, which shall be further discussed in the conclusions.

These and the previous results imply that the multibaker map admits uncountably many stationary states *for a boundary condition imposed at the level of the intercell distribution.* Indeed, uncountably many distributions are possible if we specify two numbers like $G(0, 1, 1)$ and $G(N, 1, 1)$ at both ends of a chain of length N, or the constants A_1 and A_2 in (4.11), or B_1 and B_2 in (4.13). Such boundary conditions may be considered as coarse-grained boundary conditions in which only an averaged value is imposed on the distribution. However, as in the case of several dynamical systems,[15,16,28,29] every one of these measures is not physically realizable. Several criteria have been proposed in order to select the physical measures[15,16] such as the Kolmogorov condition of maximal KS entropy for uniformly hyperbolic systems and the SRB condition of extremum of Ruelle's topological pressure for nonuniformly hyperbolic systems. In closed and finite systems, the SRB condition implies Pesin's equality that

$$h_{KS} = \sum (\text{positive Lyapunov exponents}) \tag{5.7}$$

In closed and finite systems, the previous condition selects a unique invariant measure. In the context of open and infinite systems, we observe that Pesin's equality is satisfied by two stationary states, one obeying the Fick law and the other one obeying the anti-Fick law: $h_{KS}(B, \mu_{1/2}) = h_{KS}(B, \bar{\mu}_{1/2}) = \ln 2$ [cf. Eqs. (4.20) and (4.21)]. Accordingly, the lone Pesin equality does not guarantee the unicity of the invariant measure in the context of open and infinite systems we describe here. In order to overcome this difficulty and to select the physical measure, the time evolution of an open multibaker chain of scattering type is studied in the next section, where we consider fine-grained boundary conditions in which the cumulative function is completely specified for all incoming trajectories at both ends of the chain.

6. TIME EVOLUTION OF MULTIBAKER CHAIN UNDER FIXED BOUNDARY CONDITIONS

6.1. The Map

The map B' to be considered consists of a multibaker chain of length N, both ends of which are connected with a simple shift map modeling free motion (Fig. 6):

$$B'(n,x,y)=\begin{cases}\left(n-1,2x,\dfrac{y}{2}\right), & 0\leqslant x<\dfrac{1}{2},\\ \left(n+1,2x-1,\dfrac{y+1}{2}\right), & \dfrac{1}{2}\leqslant x<1,\end{cases} \qquad 1\leqslant n\leqslant N-1 \quad (6.1a)$$

$$B'(n,x,y)=\begin{cases}(n-1,x,y), & 0\leqslant x<\dfrac{1}{2},\\ \left(n+1,2x-1,\dfrac{y+1}{2}\right), & \dfrac{1}{2}\leqslant x<1,\end{cases} \qquad n=0,-1 \quad (6.1b)$$

$$B'(n,x,y)=\begin{cases}\left(n-1,2x,\dfrac{y}{2}\right), & 0\leqslant x<\dfrac{1}{2},\\ (n+1,x,y), & \dfrac{1}{2}\leqslant x<1,\end{cases} \qquad n=N,N+1 \quad (6.1c)$$

$$B'(n,x,y)=\begin{cases}(n-1,x,y), & 0\leqslant x<\dfrac{1}{2},\\ (n+1,x,y), & \dfrac{1}{2}\leqslant x<1,\end{cases} \qquad n\leqslant -2 \text{ or } n\geqslant N+2 \quad (6.1d)$$

The first line corresponds to the multibaker transformation in the finite chain $1\leqslant n\leqslant N-1$, where the motion is dynamically unstable with a positive Lyapunov exponent ln 2 and where transport occurs by deterministic diffusion. The fourth line models a free motion of particles transported with velocities ± 1 either to the left or to the right. The second and third lines define the way by which the finite multibaker chain is coupled to the ingoing and outgoing exit channels. This system is of scattering type because particles are allowed to enter and exit the scattering region $1\leqslant n\leqslant N-1$ where the motion is nontrivial. In the limit where $N\to\infty$ and the origin $n=0$ is removed to $-\infty$, the infinite multibaker map B is recovered.

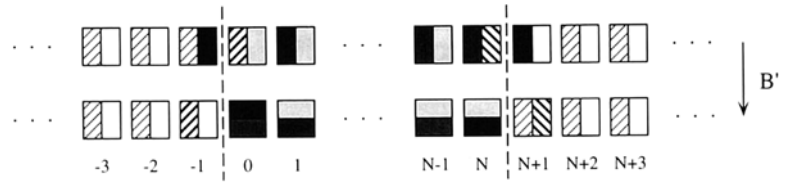

Fig. 6. Action of the open multibaker map B' defined by Eq. (6.1) on its phase space composed of an infinite chain of squares.

6.2. Equation of Motion

We now study the Liouvillian dynamics of this system in the same way as we treated the infinite chain in the previous sections. Since the inverse of B' is

$$B'^{-1}(n, x, y) = \begin{cases} \left(n+1, \frac{x}{2}, 2y\right), & 0 \leqslant y < \frac{1}{2}, \\ \left(n-1, \frac{x+1}{2}, 2y-1\right), & \frac{1}{2} \leqslant y < 1, \end{cases} \quad 0 \leqslant n \leqslant N \tag{6.2}$$

$$B'^{-1}(n, x, y) = \begin{cases} (n+1, x, y), & 0 \leqslant x < \frac{1}{2}, \\ (n-1, x, y), & \frac{1}{2} \leqslant x < 1, \end{cases} \quad n \leqslant -1 \text{ or } n \geqslant N+1$$

the equation of motion for the cumulative function $G_t(n, x, y) \equiv \mu_t(\{[0, x) \times [0, y)\}_n)$ with μ_t a measure at time t is given by

$$G_{t+1}(n, x, y) = \begin{cases} G_t\left(n+1, \frac{x}{2}, 2y\right), & 0 \leqslant y < \frac{1}{2}, \\ G_t\left(n+1, \frac{x}{2}, 1\right) + G_t\left(n-1, \frac{x+1}{2}, 2y-1\right) & \\ \quad - G_t\left(n-1, \frac{1}{2}, 2y-1\right), & \frac{1}{2} \leqslant y \leqslant 1 \end{cases} \tag{6.3a}$$

for $0 \leqslant n \leqslant N$, and

$$G_{t+1}(n, x, y) = \begin{cases} G_t(n+1, x, y), & 0 \leqslant x < \frac{1}{2} \\ G_t\left(n+1, \frac{1}{2}, y\right) + G_t(n-1, x, y) - G_t\left(n-1, \frac{1}{2}, y\right), & \frac{1}{2} \leqslant x \leqslant 1 \end{cases} \tag{6.3b}$$

for $n \leqslant -1$ or $n \geqslant N+1$.

We propose a gedanken experiment where a flow is induced across the system by imposing two different concentrations at both ends of the

system. Accordingly, we assume at the initial time two ingoing flows of particles from the left- and right-hand ends of the chain with uniform concentrations ρ_- and ρ_+, respectively:

$$\begin{aligned} G_0(n, x, y) &= \rho_- xy, \qquad n \leqslant -1 \\ G_0(n, x, y) &= \rho_+ xy, \qquad n \geqslant N+1 \end{aligned} \tag{6.4}$$

Then, the equation of motion (6.3) can be further simplified. As easily seen, (6.3b) and (6.4) lead to

$$\begin{aligned} G_t(n, x, y) - G_t(n, \tfrac{1}{2}, y) &= \rho_-(x - \tfrac{1}{2})\, y, \qquad 1 \geqslant x \geqslant \tfrac{1}{2}, \quad n \leqslant -1 \\ G_t(n, x, y) &= \rho_+ xy, \qquad 0 \leqslant x \leqslant \tfrac{1}{2}, \quad n \geqslant N+1 \end{aligned} \tag{6.5}$$

Thus, for $n = 0$ and $n = N$, we have

$$G_{t+1}(0, x, y) = \begin{cases} G_t\left(1, \dfrac{x}{2}, 2y\right), & 0 \leqslant y < \dfrac{1}{2} \\ G_t\left(1, \dfrac{x}{2}, 1\right) + \rho_- x\left(y - \dfrac{1}{2}\right), & \dfrac{1}{2} \leqslant y \leqslant 1 \end{cases} \tag{6.6a}$$

and

$$G_{t+1}(N, x, y) = \begin{cases} \rho_+ xy, & 0 \leqslant y < \dfrac{1}{2} \\ \rho_+ \dfrac{x}{2} + G_t\left(N-1, \dfrac{x+1}{2}, 2y-1\right) & \\ \qquad - G_t\left(N-1, \dfrac{1}{2}, 2y-1\right), & \dfrac{1}{2} \leqslant y \leqslant 1 \end{cases} \tag{6.6b}$$

We note that the set formed by Eqs. (6.3a) with $n = 1, 2, \ldots, N-1$ together with Eqs. (6.6) is a closed system of equations for the unknown functions $G_t(n, x, y)$ $(n = 0, 1, \ldots, N)$.

6.3. Asymptotic State

Provided that the initial state G_0 is twice continuously differentiable in x, we can show that the solution of the equations of motion (6.3a) and (6.6) asymptotically approaches the stationary state with a constant

intercell gradient and that this solution obeys Fick's law (cf. the next subsection):

$$G_\infty(n, x, y) = x\left\{\frac{\rho_+ - \rho_-}{N+2}[(n+1)y + T_n(y)] + \rho_- y\right\} \tag{6.7}$$

$$J_{n|n+1} = -\frac{1}{2}\frac{\rho_+ - \rho_-}{N+2} = -\frac{1}{2}[G_\infty(n+1, 1, 1) - G_\infty(n, 1, 1)] \tag{6.8}$$

where $\{T_n(y)\}$ are incomplete Takagi functions defined by the multiple functional equation

$$T_n(y) = \begin{cases} \frac{1}{2}T_{n+1}(2y) + y, & 0 \leqslant y < \frac{1}{2} \\ \frac{1}{2}T_{n-1}(2y-1) + 1 - y, & \frac{1}{2} \leqslant y \leqslant 1 \end{cases} \tag{6.9}$$

where $0 \leqslant n \leqslant N$ with conventions $T_{-1}(y) = T_{N+1}(y) \equiv 0$. As discussed in Appendix B, the functional equation (6.9) admits a unique continuous solution satisfying

$$\max_{0 \leqslant n \leqslant N} \|T_n\|_\infty \leqslant 1 \tag{6.10}$$

with

$$\|T_n\|_\infty \equiv \sup_{\substack{0 \leqslant x \leqslant 1 \\ 0 \leqslant y \leqslant 1}} |T_n(y)|$$

In addition, we have for $k = \max(n, N-n)$,

$$\|T_n - T\|_\infty \leqslant (\tfrac{1}{2})^{k-1} \tag{6.11}$$

where T is the complete Takagi function, solution of Eq. (4.14). The inequality (6.11) implies that, if the lattice site n is far from the ends of the chain, the incomplete Takagi function T_n is getting close to the Takagi function and the stationary state (4.13) obtained in Section 4 is recovered from the middle part of the asymptotic state (6.7) in the limit $N \to \infty$. The incomplete Takagi functions $\{T_n(y)\}$ for a chain of length $N = 10$ are shown in Fig. 7, where we observe that the distribution $T_5(y)$ at the middle site practically coincides with the Takagi function shown in Fig. 4.

The fact that the state G_∞ obeys Fick's law immediately follows from (5.1):

$$\begin{aligned} J_{n|n+1} &= G_\infty(n, 1, 1) - G_\infty\left(n, \frac{1}{2}, 1\right) - G_\infty\left(n+1, \frac{1}{2}, 1\right) \\ &= -\frac{1}{2}\frac{\rho_+ - \rho_-}{N+2} = -\frac{1}{2}[G_\infty(n+1, 1, 1) - G_\infty(n, 1, 1)] \end{aligned}$$

We reach the conclusion that the fine-grained boundary conditions considered in this section have uniquely selected the physical state obeying Fick's law out of the uncountable set of states obtained in the previous section where only coarse-grained boundary conditions were imposed.

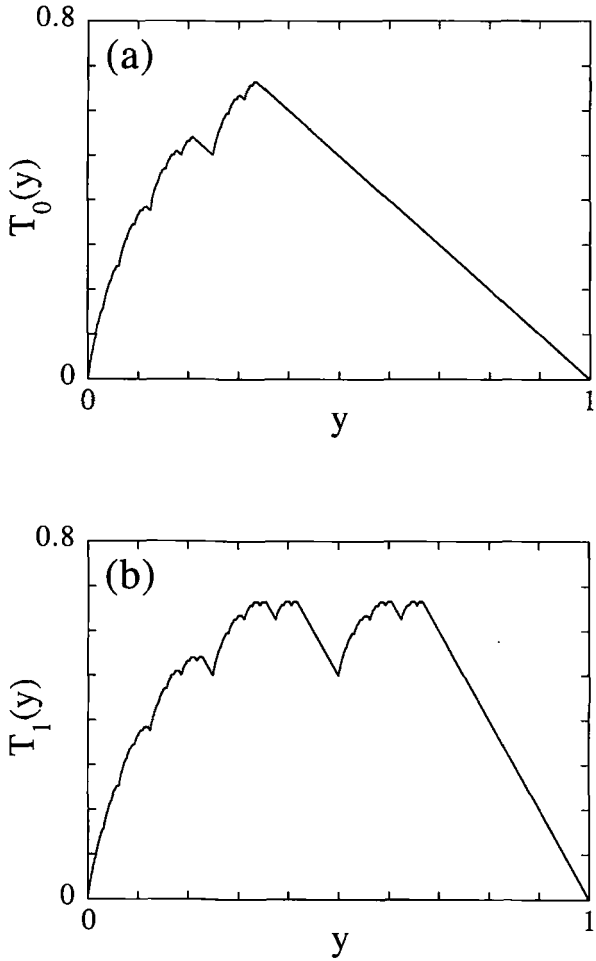

Fig. 7. The incomplete Takagi functions $\{T_n(y)\}$ given by Eqs. (6.9) along an open multi-baker chain of length $N = 10$: (a) $n = 0$; (b) $n = 1$; (c) $n = 2$; (d) $n = 3$; (e) $n = 4$; (f) $n = 5$. On the right-hand side of the chain, the same functions are obtained up to the reflection $y \to 1 - y$ because of the symmetry $T_n(y) = T_{N-n}(1 - y)$.

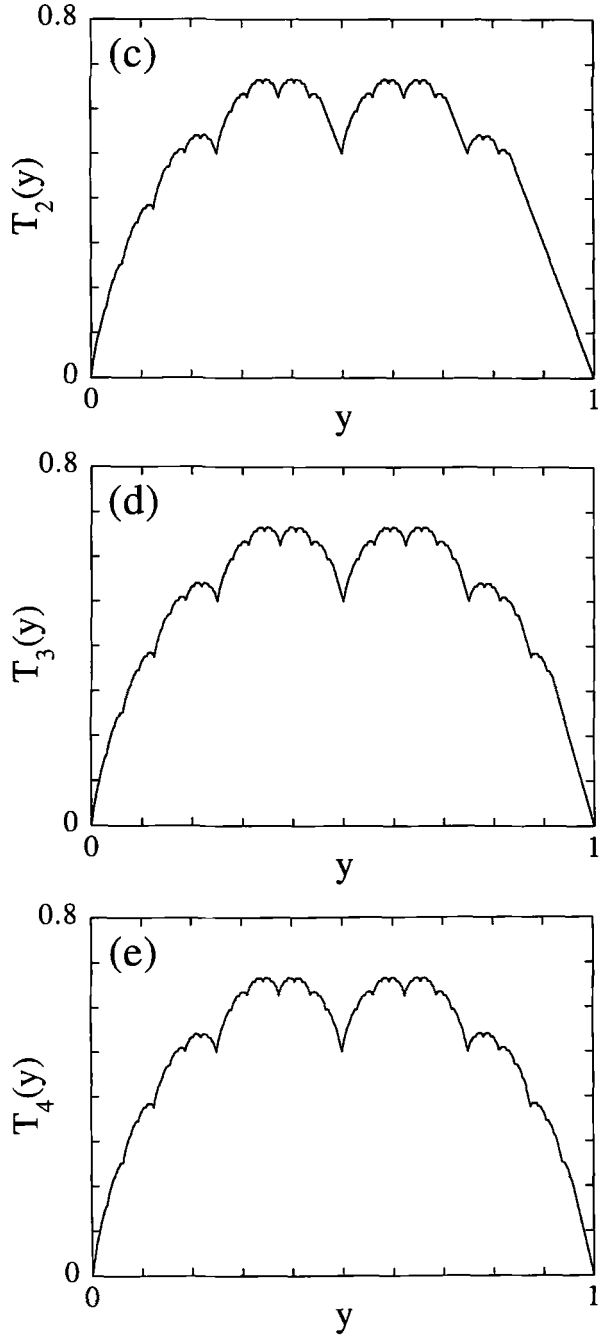

Fig. 7 (*continued*)

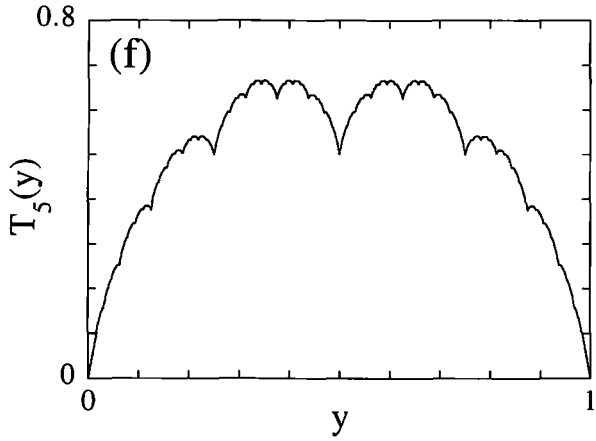

Fig. 7 (*continued*)

6.4. Convergence to the Asymptotic State

In this subsection, we show how the time evolution is responsible for the convergence of G_t to G_∞ for $t \to +\infty$ for initial conditions G_0 which are twice differentiable with respect to x. Here we outline the steps of the proof which have a well-defined physical interpretation, whereas the details are presented in Appendix C.

6.4.1. Uniformization of the Distribution Along the Unstable Direction. First, we observe that the forward time evolution given by Eqs. (6.3a) and (6.6) keeps the smoothness in the unstable x direction, i.e., if G_t is twice continuously differentiable with respect to x, G_{t+1} is also a twice continuously differentiable function of x. Then, as shown in Appendix C, the second-order derivative $\partial_x^2 G_t$ of the cumulative function obeys the inequality [cf. (C.2)]

$$\|\partial_x^2 G_t\| \leqslant (\tfrac{1}{2})^t \|\partial_x^2 G_0\| \tag{6.12}$$

with

$$\|\partial_x^2 G_t\| \equiv \max_{0 \leqslant n \leqslant N} \sup_{\substack{0 \leqslant x \leqslant 1 \\ 0 \leqslant y \leqslant 1}} |\partial_x^2 G_t(n, x, y)| \tag{6.13}$$

and thus the second-order derivative $\partial_x^2 G_t$ tends to zero asymptotically: $\partial_x^2 G_t \to 0$ $(t \to +\infty)$. This process corresponds to the uniformization of the distribution along the unstable direction.

6.4.2. Achievement of the Uniform-Gradient Intercell Distribution via Diffusion. We rewrite

$$G_t(n, x, y) = xG_t(n, 1, y) + x\delta_t(n, x, y) \tag{6.14a}$$

where

$$\delta_t(n, x, y) \equiv \frac{1}{x}\int_0^x dx' \int_0^{x'} dx''\, \partial_{x''}^2 G_t(n, x'', y) - \int_0^1 dx' \int_0^{x'} dx''\, \partial_{x''}^2 G_t(n, x'', y) \tag{6.14b}$$

and, as shown in Appendix C, it vanishes exponentially for $t \to +\infty$ [cf. (C.4)]:

$$|\delta_t(n, x, y)| \leqslant (\tfrac{1}{2})^t \, \|\partial_x^2 G_0\| \tag{6.14c}$$

By setting $x = y = 1$ in (6.3a) and (6.6) and using (6.14a), we get, for $0 \leqslant n \leqslant N$,

$$G_{t+1}(n, 1, 1) = \tfrac{1}{2}[G_t(n-1, 1, 1) + G_t(n+1, 1, 1)] + \eta_t(n) \tag{6.15a}$$

where we use the convention $G_t(-1, 1, 1) = \rho_-$, $G_t(N+1, 1, 1) = \rho_+$, and the last term $\eta_t(n)$ is a function of δ_t satisfying [cf. (C.6)]

$$|\eta_t(n)| \leqslant (\tfrac{1}{2})^t \, \|\partial_x^2 G_0\| \tag{6.15b}$$

Equation (6.15a) is precisely the random walk equation with a damped "noise" η_t.

As shown in Appendix C, the solution of (6.15a) is

$$G_t(n, 1, 1) - \left[\frac{\rho_+ - \rho_-}{N+2}(n+1) + \rho_-\right] = \frac{2}{N+2}\sum_{m=1}^{N+1} \sin\left(\frac{n+1}{N+2}\pi m\right) \times \left[\left(\cos\frac{\pi m}{N+2}\right)^t \hat{h}_0(m) + \sum_{s=1}^{t}\left(\cos\frac{\pi m}{N+2}\right)^{s-1} \hat{\eta}_{t-s}(m)\right] \tag{6.16a}$$

where $\hat{\eta}_t(m)$ and $\hat{h}_0(m)$ are the Fourier transforms, respectively, of the "noise" and of the initial deviation of $G_t(n, 1, 1)$ from the uniform-gradient distribution:

$$\hat{\eta}_t(m) = \sum_{n=0}^{N} \sin\left(\frac{n+1}{N+2}\pi m\right) \eta_t(n) \tag{6.16b}$$

$$\hat{h}_0(m) = \sum_{n=0}^{N} \sin\left(\frac{n+1}{N+2}\pi m\right) \left\{ G_0(n, 1, 1) - \left[\frac{\rho_+ - \rho_-}{N+2}(n+1) + \rho_- \right] \right\} \tag{6.16c}$$

As seen from (6.16), the intercell distribution $G_t(n, 1, 1)$ asymptotically approaches the uniform-gradient state:

$$\left| G_t(n, 1, 1) - \left[\frac{\rho_+ - \rho_-}{N+2}(n+1) + \rho_- \right] \right| \leqslant K\gamma_0^t \tag{6.17a}$$

where K is a positive constant depending on the initial deviation as well as on the initial value of the second-order derivative of the cumulative function $\partial_x^2 G_0$ [cf. (C.15)], and the decay rate γ_0 is given by

$$\gamma_0 = \cos\frac{\pi}{N+2} \quad (<1) \tag{6.17b}$$

We notice that the decay rate γ_0 coincides with the slowest decay rate via diffusion for the finite chain of length $N+2$. Hence, we conclude that the approach of the intercell distribution to the uniform-gradient state is due to the diffusion process.

6.4.3. Achievement of the Distribution in the Stable Direction. We turn to the full equation of motion (6.3a) and (6.6). By substituting (6.14a) into (6.3a) and (6.6), and setting $x = 1$ in the results, we obtain

$$G_{t+1}(n, 1, y) = \mathscr{T}_2 G_t(n, 1, y) + \delta G_t(n, 1, y) + \xi_t(n, y) \tag{6.18a}$$

where the transformation $\mathscr{T}_2$ is defined by

$$\mathscr{T}_2 f(n, y) \equiv \begin{cases} \dfrac{1}{2} f(n+1, 2y), & 0 \leqslant y < \dfrac{1}{2} \\ \dfrac{1}{2} f(n-1, 2y-1) + \dfrac{\rho_+ - \rho_-}{2(N+2)}(n+2) + \dfrac{\rho_-}{2}, & \dfrac{1}{2} \leqslant y \leqslant 1 \end{cases} \tag{6.18b}$$

for $0 \leqslant n \leqslant N$ with $f(-1, y) = \rho_- y$ and $f(N+1, y) = \rho_+ y$. The deviation $\delta G_t(n, 1, y)$ is related to the deviation of the intercell distribution with respect to the uniform-gradient state and decays via diffusion [cf. (C.18)]:

$$|\delta G_t(n, 1, y)| \leqslant \frac{K}{2} \gamma_0^t \tag{6.18c}$$

On the other hand, the "noise" ξ_t arising from the nonuniformity of the distribution along the unstable direction also decays exponentially, but at the faster rate [cf. (C.19)]

$$|\xi_t(n, y)| \leqslant (\tfrac{1}{2})^t \, \|\partial_x^2 G_0\| \tag{6.18d}$$

determined by the Lyapunov exponent $\lambda = \ln 2$.

Since the map $\mathscr{T}_2$ is a contraction

$$\|\mathscr{T}_2 f - \mathscr{T}_2 g\| \leqslant \tfrac{1}{2} \|f - g\| \tag{6.19}$$

it admits a unique fixed point $\mathscr{G}_\infty(n, y)$. The deviation of $G_t(n, 1, y)$ from $\mathscr{G}_\infty(n, y)$ obeys

$$\begin{aligned}
\|G_t(\cdot, 1, \cdot) - \mathscr{G}_\infty\| &\leqslant \|\mathscr{T}_2 G_{t-1}(\cdot, 1, \cdot) - \mathscr{T}_2 \mathscr{G}_\infty\| + \|\delta G_{t-1}\| + \|\xi_{t-1}\| \\
&\leqslant \frac{1}{2} \|G_{t-1}(\cdot, 1, \cdot) - \mathscr{G}_\infty\| + K' \gamma_0^{t-1} \\
&\leqslant \left(\frac{1}{2}\right)^t \|G_0(\cdot, 1, \cdot) - \mathscr{G}_\infty\| + K' \gamma_0^{t-1} \sum_{s=0}^{t-1} \left(\frac{1}{2\gamma_0}\right)^s \\
&\leqslant \left(\frac{1}{2}\right)^t \|G_0(\cdot, 1, \cdot) - \mathscr{G}_\infty\| + K' \frac{2\gamma_0^t}{2\gamma_0 - 1}
\end{aligned} \tag{6.20}$$

where we used Eqs. (6.18c), (6.18d), and (6.19), the fact that $\gamma_0 > 1/2$, and the positive constant

$$K' = \frac{K}{2} + \|\partial_x^2 G_0\| \tag{6.21}$$

The inequality (6.20) implies the convergence of the cumulative function $G_t(n, x, y)$ to $x\mathscr{G}_\infty(n, y)$ for $t \to \infty$:

$$\begin{aligned}
&|G_t(n, x, y) - x\mathscr{G}_\infty(n, y)| \\
&\quad \leqslant \|G_t(\cdot, 1, \cdot) - \mathscr{G}_\infty\| + |\delta_t(n, x, y)| \\
&\quad \leqslant \left(\frac{1}{2}\right)^t \|G_0(\cdot, 1, \cdot) - \mathscr{G}_\infty\| + K' \frac{2\gamma_0^t}{2\gamma_0 - 1} \\
&\qquad + \left(\frac{1}{2}\right)^t \|\partial_x^2 G_0\| \to 0, \qquad t \to +\infty
\end{aligned} \tag{6.22}$$

Straightforward calculations show that the fixed point $\mathscr{G}_\infty(n, y)$ of the contraction $\mathscr{T}_2$ is given by

$$\mathscr{G}_\infty(n, y) = \frac{\rho_+ - \rho_-}{N+2} [(n+1)y + T_n(y)] + \rho_- y$$

where the $T_n(y)$ are the incomplete Takagi functions $T_n(y)$, the solution of Eq. (6.9), whereupon the asymptotic state $x\mathscr{G}_\infty(n, y)$ is equal to G_∞ given by (6.7). This completes the proof of the convergence of G_t to G_∞.

6.5. Summary

In summary, we showed that, for $t \to +\infty$, the distribution approaches the stationary state with a uniform gradient, which obeys Fick's law. As time evolves, the distribution first becomes uniform along the unstable direction on a short kinetic time scale given by the inverse of the Lyapunov exponent (corresponding to a decay rate of ln 2). Thereafter, the linear concentration profile is achieved through diffusion on a longer hydrodynamic time scale given by the rate of escape out of the finite chain [corresponding to the decay rate $-\ln \cos(\pi/(N+2))$].

It should be noticed that the other stationary states, which are singular in the unstable direction, could also be realized in principle as asymptotic states if appropriate boundary and initial conditions are imposed. For example, through the same arguments as in Section 6.4, it can shown that the initial condition

$$G_0(n, x, y) = \begin{cases} \int_0^x df_\alpha(x')\, \rho_0(n, x', y), & 0 \leqslant n \leqslant N \\ \rho_- f_\alpha(x) f_\alpha(y), & n \leqslant -1 \\ \rho_+ f_\alpha(x) f_\alpha(y), & n \geqslant N+1 \end{cases} \tag{6.23}$$

where f_α is the solution of the deRham equation (4.9) and where the density $\rho_0(n, x, y)$ is continuously differentiable in x, tends to a stationary distribution with the exponential intercell profile (4.11) for $t \to \infty$. As we see in (6.23), the initial condition must be singular in the unstable direction in order to obtain a stationary distribution, and this fact can be understood as follows. The multibaker map B' has a tendency to uniformize the distribution along the unstable direction. Therefore, the maintenance of a stationary state which is singular in the unstable direction requires the self-similarity of the initial states along the unstable direction in order to prevent the uniformization. This observation implies that, except for very special initial states prepared to be self-similar, almost all initial states

converge to the one which is smooth in the unstable direction, and which obeys Fick's law. In other words, the Fickian stationary state is stable in this sense and we may therefore identify this state as the physical one.

7. ESCAPE-TIME FUNCTION AND THE INCOMPLETE TAKAGI FUNCTIONS

As we mentioned earlier, the open multibaker chain is of scattering type. Recently, many works have been devoted to chaotic scattering systems for which the classical dynamics has chaotic transient motions in the scattering region of phase space.[30] In this context, the trajectories which are indefinitely trapped in the scattering region form a so-called fractal repeller, which is evidenced by constructing the escape-time function. This function gives the time taken by the particle to escape from the scattering region versus its initial condition. The escape time becomes infinite on the Cantor set formed by the stable manifolds of the fractal repeller.

In the present section, we show that there is an interesting relation between the derivatives of the incomplete-Takagi-type functions and the escape-time function for a finite multibaker chain of length $N+1$. The escape time $\tau(n, x, y)$ for a given point (n, x, y) $(0 \leqslant n \leqslant N)$ is defined as the minimum number of iterations of the multibaker map B for which the initial point (n, x, y) is mapped outside of the chain. Let $(n_t, x_t, y_t) \equiv B^t(n, x, y)$; we have the defining property that

$$\begin{aligned} &0 \leqslant n_t \leqslant N && \text{for} \quad 0 \leqslant t < \tau(n, x, y) \\ &n_t = -1 \text{ or } n_t = N+1 && \text{for} \quad t = \tau(n, x, y) \end{aligned} \tag{7.1}$$

Clearly, $\tau(n, x, y) = \tau[B(n, x, y)] + 1$ for $0 \leqslant n \leqslant N$, and the points in the half-square $[0, 1/2) \times [0, 1)$ of the 0th cell and those in the half-square $[1/2, 1) \times [0, 1)$ of the Nth cell are mapped out of the chain by one iteration of B. Therefore, we have

$$\tau(n, x, y) = \begin{cases} \tau\left(n-1, 2x, \dfrac{y}{2}\right) + 1, & 0 \leqslant x < \dfrac{1}{2}, \quad 0 < n < N \\ \tau\left(n+1, 2x-1, \dfrac{y+1}{2}\right) + 1, & \dfrac{1}{2} \leqslant x < 1, \quad 0 < n < N \\ 1, & 0 \leqslant x < \dfrac{1}{2}, \quad n = 0 \\ 1, & \dfrac{1}{2} \leqslant x < 1, \quad n = N \end{cases} \tag{7.2}$$

As easily seen, the escape-time function τ is independent of y: $\tau(n, x, y) = \tau(n, x)$. We now rewrite (7.2) as an equation for the integrated escape-time function:

$$R(n, x) \equiv \int_0^x dx' \, \tau(n, x') \tag{7.3}$$

which represents the escape time averaged over the set $\{[0, x) \times [0, 1)\}_n$ in the nth cell. By simple calculations, we obtain

$$R(n, x) = \begin{cases} \frac{1}{2}R(n-1, 2x) + x, & 0 \leqslant x < \frac{1}{2}, \quad 0 \leqslant n \leqslant N \\ \frac{1}{2}R(n-1, 1) + \frac{1}{2}R(n+1, 2x-1) + x, & \frac{1}{2} \leqslant x \leqslant 1, \quad 0 \leqslant n \leqslant N \end{cases} \tag{7.4}$$

with the boundary conditions $R(-1, x) = R(N+1, x) = 0$. By setting $x = 1$, we get

$$R(n, 1) = \tfrac{1}{2}R(n-1, 1) + \tfrac{1}{2}R(n+1, 1) + 1 \tag{7.5}$$

which, together with $R(-1, 1) = R(N+1, 1) = 0$, leads to the following expression for the escape time averaged over the nth cell:

$$R(n, 1) = -(n+1)(n-N-1) \tag{7.6}$$

Hence, one can solve the full equation (7.4) by setting

$$R(n, x) = -(n+1)(n-N-1)\, x + (2n-N)\, \tilde{T}_n(x) + S_n(x) \tag{7.7a}$$

where the new functions $\tilde{T}_n(x)$ and $S_n(x)$ are defined as solutions of the following functional equations:

$$\tilde{T}_n(x) = \begin{cases} \frac{1}{2}\tilde{T}_{n-1}(2x) + x, & 0 \leqslant x < \frac{1}{2} \\ \frac{1}{2}\tilde{T}_{n+1}(2x-1) + 1 - x, & \frac{1}{2} \leqslant x \leqslant 1 \end{cases} \tag{7.7b}$$

$$S_n(x) = \begin{cases} \frac{1}{2}S_{n-1}(2x) - \tilde{T}_{n-1}(2x), & 0 \leqslant x < \frac{1}{2} \\ \frac{1}{2}S_{n+1}(2x-1) + \tilde{T}_{n+1}(2x-1), & \frac{1}{2} \leqslant x \leqslant 1 \end{cases} \tag{7.7c}$$

with the convention $\tilde{T}_{-1}(x) = \tilde{T}_{N+1}(x) \equiv 0$ and $S_{-1}(x) = S_{N+1}(x) \equiv 0$. The uniqueness and the continuity of $\tilde{T}_n(x)$ and $S_n(x)$ follow from Theorem B of Appendix B by setting, respectively,

$$w_n(x) = \begin{cases} x, & 0 \leqslant x < \frac{1}{2} \\ 1 - x, & \frac{1}{2} \leqslant x \leqslant 1 \end{cases} \tag{7.8a}$$

$$w_n(x) = \begin{cases} -\tilde{T}_{n-1}(2x), & 0 \leqslant x < \frac{1}{2} \\ \tilde{T}_{n+1}(2x-1), & \frac{1}{2} \leqslant x \leqslant 1 \end{cases} \tag{7.8b}$$

The function $\tilde{T}_n$ is essentially the incomplete Takagi function T_n:

$$\tilde{T}_n(x) = T_n(1-x) \tag{7.9}$$

As we see from the functional equation (7.7c), the other function S_n is also of Takagi type. When the site coordinate n is far from the edges, the functions $\tilde{T}_n$ and S_n converge respectively to the Takagi function $T(1-x) = T(x)$ and to the function $S(x)$ defined by

$$S(x) = \begin{cases} \frac{1}{2}S(2x) - T(2x), & 0 \leqslant x < \frac{1}{2} \\ \frac{1}{2}S(2x-1) + T(2x-1), & \frac{1}{2} \leqslant x \leqslant 1 \end{cases} \tag{7.10}$$

As a consequence of the nowhere differentiability of the functions T and S, the functions $\tilde{T}_n$ and S_n have infinite derivatives more frequently when n is far from the edges than when n is close to the edges. This property corresponds to the existence of many more trapped trajectories inside the chain than near the edges. In this respect, the singular nature of the incomplete-Takagi-type functions is closely related to the singularities of the escape-time function.

This fact can also be seen in the Hausdorff measure of the set Φ of phase-space points with infinite escape time, which is formed by the stable manifolds of the repeller. Since the multibaker map is uniformly hyperbolic, the set Φ is a Cantor set with a single scale and, as shown in Appendix D, its Hausdorff dimension D_H is [cf. (D.11)]

$$D_H = 2 + \frac{\ln \cos[\pi/(N+2)]}{\ln 2} \tag{7.11}$$

The corresponding Hausdorff measure of the intersection of Φ with the kth cell $\{[0,1]^2\}_k$ depends sinusoidally on the cell coordinate k [cf. (D.12)]:

$$\mu_H(\Phi \cap \{[0,1]^2\}_k) \propto \sin\left(\frac{k+1}{N+2}\pi\right) \tag{7.12}$$

which implies that the trapped trajectories are denser inside the chain than near the edges.

Figure 8 shows the integrated escape-time function R. The escape-time function τ obtained as the numerical derivative of R is depicted in Fig. 9 and compared with the one directly calculated from the trajectories in a chain of length $N = 10$. As seen in Fig. 9, the result of the functional equations (7.7) and the direct one agree quite well for small n. For $n = 5$ at the middle of the chain, the escape-time functions obtained from both methods oscillate around the average value of $\langle \tau \rangle \sim 36$, which agrees well with the analytic result (7.6). Indeed, the latter gives $\langle \tau \rangle = R(5,1) = 36$ for $N = 10$

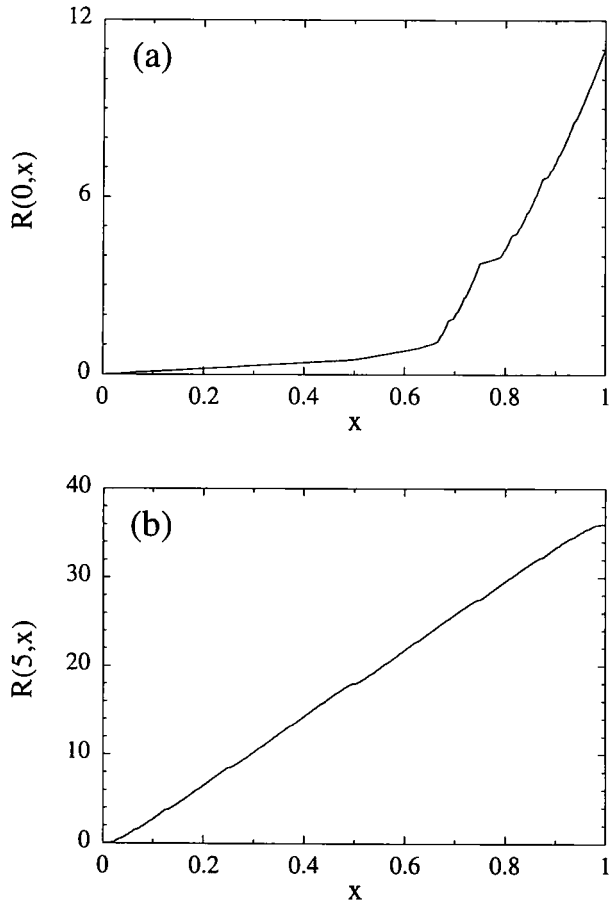

Fig. 8. The integrated escape-time function $R(n, x)$ solution of Eqs. (7.4)–(7.7) along an open multibaker chain of length $N = 10$: (a) at the left-hand end, $n = 0$; (b) in the middle, $n = 5$.

and $n = 5$. However, the agreement between the escape-time functions calculated from the two methods deteriorates as the escape time increases. Consequently, a discrepancy appears at the level of the integrated escape-time function $R(n, x)$, which, in the direct method, is obtained via numerical integration. The discrepancy arises from the very slow convergence of the numerical integration due to the singularities of the escape time distribution $\tau(n, x)$, as explained below.

First, we consider the singularities of the escape-time function near a single repelling point. Let x_0 be this repelling point. Nearby initial points

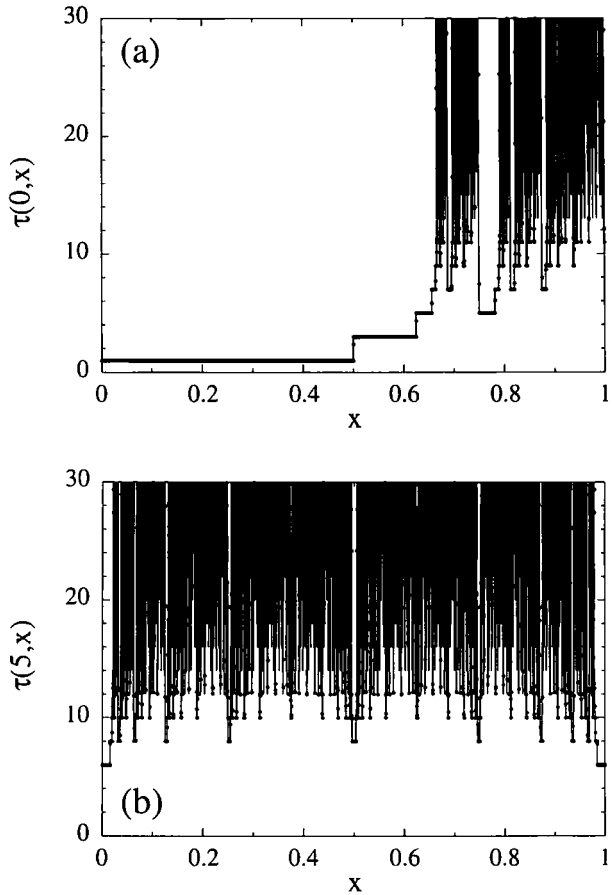

Fig. 9. The escape-time function $\tau(n, x)$ along an open multibaker chain of length $N = 10$: (a) at the left-hand end, $n = 0$; (b) in the middle, $n = 5$. The solid line represents the direct calculation by trajectory integration according to the definition given by Eq. (7.1). The dots are the results of a numerical differentiation of the function $R(n, x)$ plotted in Fig. 8.

like $x = x_0 + \delta x$ escape from the vicinity of the repeller x_0 at a rate given by the Lyapunov exponent λ: $x_t = x_0 + \delta x \exp(\lambda t)$. By setting $x_t - x_0 \sim 1$, the escape time τ_{esc} of x is thus obtained as $\tau_{\text{esc}} = -\ln |x - x_0|/\lambda$. The escape-time function $\tau(n, x)$ is expected to behave in a similar way near each of its singularities. On the other hand, the set of singularities of $\tau(n, x)$ is the projection of the stable manifolds Φ of the repeller onto the x axis. Since Φ is a Cantor set with the Hausdorff dimension D_{H}, (7.11), and takes

the form $\Phi = \bigcup_k \{\mathscr{F}_k \times [0, 1]\}_k$, where $\mathscr{F}_k$ is a fractal set in the kth cell, the set of singularities of $\tau(n, x)$ is also a Cantor set with the dimension

$$d_H = D_H - 1 = 1 + \frac{\ln \cos[\pi/(N+2)]}{\ln 2} \tag{7.13}$$

Let us subdivide the interval $[0, x]$ with a grid of spacing δ and consider the difference ε_{NET} between the integral of τ and the corresponding Riemann sum:

$$\varepsilon_{NET} \equiv \left| \delta \sum_{j=1}^{[x/\delta]} \tau(n, j\delta) - \int_0^x dx' \, \tau(n, x') \right| \tag{7.14}$$

The error ε_{NET} mainly comes from the intervals involving singularities. For each interval involving a singularity x_0, the error ε_s can be estimated as

$$\varepsilon_s \sim \int_{x_0-\delta/2}^{x_0+\delta/2} dx' \, \frac{-\ln|x'-x_0|}{\lambda} - \delta \frac{-\ln|x-x_0|}{\lambda}\bigg|_{x=x_0-\delta/2} = \frac{\delta}{\lambda} \sim \delta \tag{7.15}$$

Since the set of singularities of τ is a Cantor set with Hausdorff dimension d_H, the number of intervals involving singularities is of order of $1/\delta^{d_H}$. Hence, the net error ε_{NET} is estimated as

$$\varepsilon_{NET} \sim \frac{1}{\delta^{d_H}} \varepsilon_s \sim \delta^{1-d_H} \tag{7.16}$$

which approaches zero very slowly for a vanishing grid spacing $\delta \to 0$ and is responsible for the aforementioned discrepancy between the functional equation approach and the direct trajectory approach. Indeed, when $N = 10$, the dimension is about $d_H \simeq 1 - 0.05$, so that the net error becomes $\varepsilon_{NET} \sim \delta^{0.05}$, which is about $\varepsilon_{NET} \sim 0.3$ even for $\delta = 10^{-10}$. The numerical convergence is therefore extremely slow in the integration of such escape-time functions.

8. CONCLUDING REMARKS

We have shown that, for the multibaker map, nonequilibrium stationary states with flow can be constructed with the aid of singular measures. By investigating the time evolution of the distribution for a finite multibaker chain under fixed boundary conditions, the one satisfying Fick's law is selected as the physical state. Some remarks are now in order.

1. In the phenomenological diffusion equation $\partial f/\partial t = D\,\partial^2 f/\partial x^2$, the decaying mode $f_q(x) = \exp(iqx)$ and the constant-gradient state $\bar{f}(x) = x$ are related to each other in a simple way:

$$\bar{f}(x) = -i\left[\frac{\partial}{\partial q} f_q(x)\right]_{q=0} \tag{8.1}$$

A similar relation holds between the state (4.13) satisfying Fick's law and the decay mode of the Frobenius–Perron operator $\hat{U}$ corresponding to the Lebesgue invariant measure. As discussed in refs. 7–9, the Frobenius–Perron operator $\hat{U}$ acts on the distribution function $\rho(n, x, y)$ as

$$\hat{U}\rho(n, x, y) = \rho[B^{-1}(n, x, y)] = \begin{cases} \rho\left(n+1, \dfrac{x}{2}, 2y\right), & 0 \leqslant y < \dfrac{1}{2} \\ \rho\left(n-1, \dfrac{x+1}{2}, 2y-1\right), & \dfrac{1}{2} \leqslant y < 1 \end{cases} \tag{8.2}$$

The operator $\hat{U}$ admits a generalized decaying eigendistribution F_q characterized by a quasimomentum q ($-\pi/3 < q < \pi/3$ or $2\pi/3 < q < 4\pi/3$)[7,12] and corresponding to the eigenvalue $\cos q$:

$$\langle A \mid F_q \rangle \equiv \sum_{n=-\infty}^{+\infty} \int_0^1 dx \int_0^1 df_{\alpha_q}(y)\, e^{inq} A^*(n, x, y) \tag{8.3}$$

where A is an arbitrary function with bounded variation with respect to y and the function f_{α_q} is a solution of the deRham equation (4.9) corresponding to a complex parameter $\alpha = \alpha_q = \exp(iq)/(2\cos q)$.

By differentiating (8.3) with respect to q and setting $q = 0$, we have

$$-i\left[\frac{\partial}{\partial q}\langle A \mid F_q \rangle\right]_{q=0} = -i \sum_{n=-\infty}^{+\infty} \int_0^1 dx \int_0^1 d\left(inf_{\alpha_0}(y) + \left[\frac{\partial}{\partial q} f_{\alpha_q}(y)\right]_{q=0}\right) A^*(n, x, y)$$

Using $f_{\alpha_0}(y) = y$ and the following relation obtained by Hata and Yamaguti[20] between the function f_α and the Takagi function $T(y)$:

$$\left[\frac{\partial}{\partial q} f_{\alpha_q}(y)\right]_{q=0} = \frac{i}{2}\left[\frac{\partial}{\partial \alpha} f_\alpha(y)\right]_{\alpha = 1/2} = iT(y)$$

we obtain the desired relation

$$-i\left[\frac{\partial}{\partial q}\langle A|F_q\rangle\right]_{q=0} = \sum_{n=-\infty}^{+\infty}\int_0^1 dx \int_0^1 d[ny+T(y)]\, A^*(n,x,y)$$

$$= \sum_{n=-\infty}^{+\infty}\int_{[0,1]\times[0,1]} dG(n,x,y)\, A^*(n,x,y)$$

where the cumulative function $G(n, x, y)$ is given by (4.13) with $B_1 = 1$ and $B_2 = 0$: $G(n, x, y) = x[ny + T(y)]$. This result shows how Fick's nonequilibrium stationary states can be directly obtained from the generalized spectral decomposition of the Frobenius–Perron operator in terms of its Pollicott–Ruelle resonances and the associated eigendistributions.

2. As shown before, the stationary state satisfying Fick's law is expressed in terms of a singular measure. Since the multibaker map is ergodic,[6] any state described by a density function, i.e., by an absolutely continuous measure with respect to the equilibrium Lebesgue measure, weakly converges to the equilibrium state and there cannot be any other stationary state. Therefore, the description in terms of density functions cannot cope with nonequilibrium stationary states. In contrast, our approach based on a direct treatment of the cumulative functions shows the existence of many nontrivial invariant measures corresponding to nonequilibrium stationary states under various boundary conditions. This observation suggests, in general, the necessity of singular measures to treat nonequilibrium stationary states in reversible and volume-preserving dynamical systems and thus the necessity to extend the description of dynamical states as we have carried out in the present paper.

3. This and the next remark concern the relationship between Fick's law and the SRB measure. The SRB measure has the property to be an ergodic invariant measure which is absolutely continuous with respect to the Lebesgue measure along the unstable direction.[15,16] For a sufficiently smooth map defined on a compact phase space, the SRB measure satisfies Pesin's equality and is moreover the ergodic invariant measure given by time averaging over almost all trajectories. The Fickian invariant state we constructed could be regarded as a kind of SRB measure since it is expressed by a measure which is absolutely continuous with respect to the Lebesgue measure in the unstable x direction [cf. (4.13) and (6.7)] and since it can be obtained, in an open multibaker chain, as an asymptotic state starting from an initial state which is absolutely continuous with respect to the Lebesgue measure (cf. the discussion in Section 6). However, the present situation concerning open and infinite systems differs on the following points from the case of closed systems. As discussed at the end

of Section 5, there appear two stationary states—the Fickian and the anti-Fickian—which both satisfy Pesin's equality. Moreover, for the open multibaker chain discussed in Section 6, different asymptotic states can be obtained, depending on the boundary conditions. Therefore, the asymptotic states are controlled not only by a dynamics, but also by the boundary conditions, as we emphasized.

4. In dynamical system theory, singular measures have been considered in the context of dissipative and, more generally, of nonconservative systems where contraction of phase space volumes naturally leads to the formation of fractal objects where the invariant measure is singular as on the Cantor set. Singular measures having a fractal support are also considered in chaotic scattering of conservative systems, as is the case in the open multibaker chain of Sections 6 and 7. We would like to draw attention to the fact that not only is the dynamics of the multibaker conservative, but the support of the invariant measures μ_α we construct and study in Sections 3–5 is the plain phase space. In spite of these features, the invariant measures μ_α are singular and belong to a class of measures which are intermediate between the measures which are absolutely continuous with respect to the Lebesgue measure and the measures supported by a fractal. By this property, the invariant measures μ_α differ from the SRB measures currently considered in the study of strange attractors. The possibility that nonequilibrium stationary states belong to this intermediate class of singular invariant measures seems to have been overlooked. Our results show that such a possibility is compatible with the conservation of volumes in phase space.

APPENDIX A. SYMBOLIC REPRESENTATION

Let $\omega = \{\omega_n\}_{-\infty < n < \infty}$ be a bilateral symbolic sequence of integers, i.e., $\omega_n \in \mathbf{Z}$. Let us define a subset Ω of the symbolic sequence space as

$$\Omega = \{\omega = \{\omega_n\}_{-\infty < n < \infty} : a_{\omega_n \omega_{n+1}} \neq 0\} \tag{A.1}$$

where a_{ij} $(i, j \in \mathbf{Z})$ is a transition matrix:

$$a_{ij} \neq 0 \qquad (\text{only for} \quad i = j \pm 1) \tag{A.2}$$

To each finite sequence $\bar{\omega} = \{\omega_n\}_{-M \leqslant n \leqslant N}$ we can associate a cylindrical set $\Sigma_{\bar{\omega}}$ which is a subset of Ω defined by

$$\Sigma_{\bar{\omega}} \equiv \{\omega' = \{\omega'_j\}_{-\infty < j < \infty} \in \Omega : \omega'_n = \omega_n \, (-M \leqslant n \leqslant N)\} \tag{A.3}$$

Then we have the following result.

Theorem A. (1) The mapping σ from the phase space $\bigcup_{-\infty<n<\infty}\{[0,1]^2\}_n$ to the symbolic sequence space Ω defined by

$$\sigma: p=(n,x,y)\to\omega=\{\omega_n\}_{-\infty<n<\infty} \quad \text{s.t.} \quad \omega_n=k \text{ iff } B^n p\in\{[0,1]^2\}_k \tag{A.4}$$

is bijective.

(2) For a finite sequence $\bar{\omega}=\{\omega_n\}_{-M\leqslant n\leqslant N}$ $(a_{\omega_n\omega_{n+1}}\neq 0)$, the measure of the preimage $\sigma^{-1}\Sigma_{\bar{\omega}}$ of a cylindrical set $\Sigma_{\bar{\omega}}$ with respect to the measure μ_α defined through the deRham-type equations (4.3) and (4.5) is given by

$$\mu_\alpha(\sigma^{-1}\Sigma_{\bar{\omega}})=G(\omega_{-M},1,1)\,P_{\omega_{-M}\omega_{-M+1}}P_{\omega_{-M+1}\omega_{-M+2}}\cdots P_{\omega_{N-1}\omega_N} \tag{A.5}$$

where P_{ij} is the transition probability defined by (4.19).

(3) The measure μ_α defined through deRham-type equations (4.3) and (4.5) induces a measure μ_α^{S} on the symbolic sequence space Ω via the mapping σ as

$$\mu_\alpha^{\mathrm{S}}(\Sigma_{\bar{\omega}})\equiv\mu_\alpha(\sigma^{-1}\Sigma_{\bar{\omega}}) \tag{A.6}$$

where $\bar{\omega}=\{\omega_n\}_{-M\leqslant n\leqslant N}$ is a finite symbolic sequence and $\Sigma_{\bar{\omega}}$ the corresponding cylindrical set. Then μ_α^{S} is a shift-invariant Markov measure on Ω. Hereafter, we sometimes abbreviate $\mu_\alpha^{\mathrm{S}}(\Sigma_{\bar{\omega}})$ as $\mu_\alpha^{\mathrm{S}}(\bar{\omega})$.

Theorem A completes the proof of the isomorphism between the multibaker map and the probabilistic Markov chain.

To get Theorem A, we need a lemma which can be proved straightforwardly by induction:

Lemma A. For a finite sequence $\bar{\omega}=\{\omega_n\}_{-M\leqslant n\leqslant N}$ $(M\geqslant 0,\ N\geqslant 0,$ $a_{\omega_n\omega_{n+1}}\neq 0)$, we have (1)

$$\sigma^{-1}\Sigma_{\bar{\omega}}=\bigcap_{n=-M}^{N}B^{-n}\{[0,1]^2\}_{\omega_n}=\{[a_N,b_N]\times[c_M,d_M]\}_{\omega_0} \tag{A.7a}$$

with

$$b_N-a_N=\frac{1}{2^N},\qquad d_M-c_M=\frac{1}{2^M} \tag{A.7b}$$

and (2)

$$\begin{aligned}&G(\omega_0,1,d_M)-G(\omega_0,1,c_M)\\&\quad=G(\omega_{-M},1,1)\,P_{\omega_{-M}\omega_{-M+1}}P_{\omega_{-M+1}\omega_{-M+2}}\cdots P_{\omega_{-1}\omega_0}\\&F(\omega_0,b_N)-F(\omega_0,a_N)=P_{\omega_0\omega_1}P_{\omega_1\omega_2}\cdots P_{\omega_{N-1}\omega_N}\end{aligned} \tag{A.8}$$

where G and F are solutions of (4.3) and (4.5), respectively, and P_{ij} is defined by (4.19).

Remark. Strictly speaking, Theorem A and Lemma A hold for a map $\tilde{B}$ modified with respect to B such that $\tilde{B}^{-j}\{[0,1]^2\}_k$ becomes a closed set. As the two maps are different on a set of μ-measure zero (a union of countably many lines, where the modified map becomes double valued), the difference is not essential.

Proof of Theorem A. (1) It is enough to show that, for arbitrary $\omega = \{\omega_n\}_{-\infty<n<\infty} \in \Omega$, the set $\sigma^{-1}\{\omega\}$ consists of a unique phase point.

We shall set

$$\Sigma_{(M,N)} \equiv \{\omega' = \{\omega'_j\}_{-\infty<j<\infty} \in \Omega: \omega'_j = \omega_j,\ j = -M, -M+1, \ldots, N\} \quad \text{(A.9)}$$

Then clearly

$$\Sigma_{(M',N')} \subset \Sigma_{(M,N)} \qquad (M' \geqslant M \text{ and } N' \geqslant N) \quad \text{(A.10a)}$$

$$\bigcap_{M=0}^{\infty} \bigcap_{N=0}^{\infty} \Sigma_{(M,N)} = \{\omega\} \quad \text{(A.10b)}$$

By Lemma A, we have

$$\sigma^{-1}\Sigma_{(M,N)} = \{[a_N, b_N] \times [c_M, d_M]\}_{\omega_0} \quad \text{(A.11a)}$$

with

$$b_N - a_N = \frac{1}{2^N} \qquad \text{and} \qquad d_M - c_M = \frac{1}{2^M} \quad \text{(A.11b)}$$

Then, as a result of (A.10a), we have

$$[a_{N'}, b_{N'}] \subset [a_N, b_N]\ (N \leqslant N'), \qquad [c_{M'}, d_{M'}] \subset [c_M, d_M]\ (M \leqslant M') \quad \text{(A.12)}$$

Equations (A.11b) and (A.12) imply that $\{[a_N, b_N]\}_{N=0,1,\ldots}$ and $\{[c_M, d_M]\}_{M=0,1,\ldots}$ are sequences of shrinking closed intervals. Therefore, there exists a unique point $(x_\infty, y_\infty) \in [0,1]^2$ such that

$$\bigcap_{N=0}^{\infty} [a_N, b_N] = \{x_\infty\}, \qquad \bigcap_{M=0}^{\infty} [c_M, d_M] = \{y_\infty\} \quad \text{(A.13)}$$

which lead to the desired result:

$$\begin{aligned}\sigma^{-1}\{\omega\} &= \sigma^{-1}\left(\bigcap_{N=0}^{\infty}\bigcap_{M=0}^{\infty}\Sigma_{(M,N)}\right)\\ &= \bigcap_{N=0}^{\infty}\bigcap_{M=0}^{\infty}\sigma^{-1}\Sigma_{(M,N)}\\ &= \left\{\bigcap_{N=0}^{\infty}[a_N, b_N]\times\bigcap_{M=0}^{\infty}[c_M, d_M]\right\}_{\omega_0}\\ &= \{(\omega_0, x_\infty, y_\infty)\}\end{aligned}$$

(2) For $M\geqslant 0$ and $N\geqslant 0$, we have from Lemma A

$$\sigma^{-1}\Sigma_{\bar{\omega}} = \{[a_N, b_N]\times[c_M, d_M]\}_{\omega_0}$$

Then, the condition of product measure (4.2) and (2) of Lemma A give the desired result:

$$\begin{aligned}\mu_\alpha(\sigma^{-1}\Sigma_{\bar{\omega}}) &= \mu_\alpha(\{[a_N, b_N]\times[c_M, d_M]\}_{\omega_0})\\ &= [G(\omega_0, 1, d_M) - G(\omega_0, 1, c_M)][F(\omega_0, b_N) - F(\omega_0, a_N)]\\ &= G(\omega_{-M}, 1, 1)\, P_{\omega_{-M}\omega_{-M+1}} P_{\omega_{-M+1}\omega_{-M+2}}\cdots P_{\omega_{N-1}\omega_N}\end{aligned} \tag{A.14}$$

Now, we consider the case with $N<0$. Let $\bar{\omega}=\{\omega_n\}_{-M\leqslant n\leqslant N}$ and $\bar{\omega}'=\{\omega'_n\}_{-M\leqslant n\leqslant N}$ be different finite sequences; then $\omega_{n'}\neq\omega'_{n'}$ for some n', and

$$B^{n'}\bigcap_{j=-M}^{N} B^{-j}\{[0,1]^2\}_{\omega_j} = \bigcap_{j=-M}^{N} B^{-j+n'}\{[0,1]^2\}_{\omega_j}\subset\{[0,1]^2\}_{\omega_{n'}} \tag{A.15a}$$

$$B^{n'}\bigcap_{j=-M}^{N} B^{-j}\{[0,1]^2\}_{\omega'_j} = \bigcap_{j=-M}^{N} B^{-j+n'}\{[0,1]^2\}_{\omega'_j}\subset\{[0,1]^2\}_{\omega'_{n'}} \tag{A.15b}$$

which gives

$$\begin{aligned}&\bigcap_{j=-M}^{N} B^{-j}\{[0,1]^2\}_{\omega_j}\cap\bigcap_{j=-M}^{N} B^{-j}\{[0,1]^2\}_{\omega'_j}\\ &\quad= B^{-n'}\left(\bigcap_{j=-M}^{N} B^{-j+n'}\{[0,1]^2\}_{\omega_j}\cap\bigcap_{j=-M}^{N} B^{-j+n'}\{[0,1]^2\}_{\omega'_j}\right)\\ &\quad= B^{-n'}\varnothing = \varnothing\end{aligned} \tag{A.16}$$

as a result of

$$\{[0,1]^2\}_{\omega_{n'}} \cap \{[0,1]^2\}_{\omega'_{n'}} = \varnothing$$

with $\varnothing$ being the empty set.

Then, we have

$$\begin{aligned}
\mu_\alpha(\sigma^{-1}\Sigma_{\bar{\omega}}) &= \mu_\alpha\left[\bigcup_{\omega_0}\bigcup_{\omega_{-1}}\cdots\bigcup_{\omega_{N+1}}\bigcap_{j=-M}^{0} B^{-j}\{[0,1]^2\}_{\omega_j}\right] \\
&= \sum_{\omega_0}\sum_{\omega_{-1}}\cdots\sum_{\omega_{N+1}}\mu_\alpha\left[\bigcap_{j=-M}^{0} B^{-j}\{[0,1]^2\}_{\omega_j}\right] \\
&= \sum_{\omega_0}\sum_{\omega_{-1}}\cdots\sum_{\omega_{N+1}} G(\omega_{-M},1,1)\,P_{\omega_{-M}\omega_{-M+1}} \\
&\quad \times P_{\omega_{-M+1}\omega_{-M+2}}\cdots P_{\omega_{N-1}\omega_N}P_{\omega_N\omega_{N+1}}\cdots P_{\omega_{-1}\omega_0} \\
&= G(\omega_{-M},1,1)\,P_{\omega_{-M}\omega_{-M+1}}P_{\omega_{-M+1}\omega_{-M+2}}\cdots P_{\omega_{N-1}\omega_N} \qquad \text{(A.17)}
\end{aligned}$$

where we have used $\bigcup_\omega B^{-j}\{[0,1]^2\}_\omega = (\text{total phase space})$, (A.16), (A.14), and $\sum_j P_{ij} = 1$, respectively, at the first, second, third, and fourth equalities.

Similarly, the statement (2) for $M < 0$ can be proved by using Eq. (4.4) instead of $\sum_j P_{ij} = 1$.

(3) The shift invariance of μ_α^{S} follows directly from the result (2). Because of

$$\mu_\alpha^{\mathrm{S}}(\omega_{-M},\omega_{-M+1},\ldots,\omega_{N-1},\omega_N) = \mu_\alpha^{\mathrm{S}}(\omega_{-M},\omega_{-M+1},\ldots,\omega_{N-1})\,P_{\omega_{N-1}\omega_N}$$

we have

$$\begin{aligned}
&\sum_{\omega_N}\mu_\alpha^{\mathrm{S}}(\omega_{-M},\omega_{-M+1},\ldots,\omega_{N-1},\omega_N) \\
&\quad = \mu_\alpha^{\mathrm{S}}(\omega_{-M},\omega_{-M+1},\ldots,\omega_{N-1})\sum_{\omega_N}P_{\omega_{N-1}\omega_N} \\
&\quad = \mu_\alpha^{\mathrm{S}}(\omega_{-M},\omega_{-M+1},\ldots,\omega_{N-1})
\end{aligned}$$

which implies the Markov property of μ_α^{S}. QED

APPENDIX B. INCOMPLETE TAKAGI FUNCTION

In this appendix, we discuss the property of the incomplete Takagi function introduced in Section 6. First, we show that the multiple functional equation (6.9) uniquely defines the incomplete Takagi function and

that it is continuous. This property appears as a special case of the following theorem:

Theorem B. Let z be x or y and let $\{w_n(z)\}$ $(n=0,..., N)$ be continuous functions of $z \in [0, 1]$ satisfying $w_n(0) = w_n(1) = 0$. We introduce a transformation $\mathcal{T}_3$ as

$$\mathcal{T}_3 g_n(z) = \begin{cases} \frac{1}{2} g_{n+1}(2z) + w_n(z), & 0 \leqslant z < \frac{1}{2} \\ \frac{1}{2} g_{n-1}(2z-1) + w_n(z), & \frac{1}{2} \leqslant z \leqslant 1 \end{cases} \tag{B.1}$$

where $n=0, 1,..., N$ with the conventions $g_{-1}(z) = g_{N+1}(z) \equiv 0$. Then, the fixed-point equation

$$\mathcal{T}_3 g_n(z) = g_n(z) \qquad (n=0, 1,..., N) \tag{B.2}$$

admits a unique solution which is continuous in z and satisfies

$$\max_{0 \leqslant n \leqslant N} \|g_n\|_\infty \leqslant 2 \max_{0 \leqslant n \leqslant N} \|w_n\|_\infty \tag{B.3}$$

with

$$\|g_n\|_\infty \equiv \sup_{0 \leqslant z \leqslant 1} |g_n(z)|$$

The multiple functional equation (6.9) for the incomplete Takagi function is a special case of the fixed-point equation (B.2) with the choice of $z = y$ and

$$w_n(y) = \begin{cases} y, & 0 \leqslant y < 1/2 \\ 1-y, & 1/2 \leqslant y \leqslant 1 \end{cases} \tag{B.4}$$

which satisfies

$$\|w_n\|_\infty \leqslant 1/2 \tag{B.5}$$

Therefore, the uniqueness and the continuity of the incomplete Takagi function follow immediately from Theorem B. Its upper bound (6.10) is a consequence of (B.3) and (B.5).

Also (6.11) holds:

$$\|T_n - T\|_\infty \leqslant (\tfrac{1}{2})^{k-1} \tag{B.6}$$

where T is the Takagi function and $k = \max(n, N-n)$. Indeed, by subtracting the functional equation (4.14) for the Takagi function from the each

member of the multiple functional equation for the incomplete Takagi function (6.9), we obtain

$$\begin{aligned}
\|T_n - T\|_\infty &\leqslant \tfrac{1}{2} \max(\|T_{n+1} - T\|_\infty, \|T_{n-1} - T\|_\infty) \\
&\leqslant \tfrac{1}{2} \max_{-1 \leqslant j \leqslant 1} \|T_{n+j} - T\|_\infty \\
&\leqslant (\tfrac{1}{2})^2 \max_{-2 \leqslant j \leqslant 2} \|T_{n+j} - T\|_\infty \\
&\leqslant \cdots \leqslant (\tfrac{1}{2})^k \max_{-k \leqslant j \leqslant k} \|T_{n+j} - T\|_\infty \\
&\leqslant (\tfrac{1}{2})^k \max_{0 \leqslant m \leqslant N} \|T_m - T\|_\infty \\
&\leqslant (\tfrac{1}{2})^k [\max_{0 \leqslant m \leqslant N} \|T_m\|_\infty + \|T\|_\infty] \\
&\leqslant (\tfrac{1}{2})^{k-1}
\end{aligned}$$

Finally, we give the proof of Theorem B:

Proof of Theorem B. Since

$$\max_{0 \leqslant n \leqslant N} \|\mathscr{T}_3 g_n - \mathscr{T}_3 g'_n\|_\infty \leqslant \tfrac{1}{2} \max_{0 \leqslant n \leqslant N} \|g_n - g'_n\|_\infty$$

the transformation $\mathscr{T}_3$ is a contraction and thus the fixed-point equation (B.2) admits a unique fixed point. It is also obvious that, if $g_n(z)$ is continuous in z and satisfies $g_n(0) = g_n(1) = 0$ for all $0 \leqslant n \leqslant N$, then $\mathscr{T}_3 g_n(z)$ possesses the same properties. Therefore, the elements of the sequence $\{\mathscr{T}_3^s q_n(z)\}$ $(s = 0, 1, \ldots)$ with $q_n(z) \equiv 0$, which uniformly converges to the fixed point of $\mathscr{T}_3$, are all continuous in z and thus the fixed point itself is continuous as a uniform limit of continuous functions. Moreover, by the definition (B.1) of the transformation $\mathscr{T}_3$, we have

$$\max_{0 \leqslant n \leqslant N} \|g_n\|_\infty = \max_{0 \leqslant n \leqslant N} \|\mathscr{T}_3 g_n\|_\infty \leqslant \tfrac{1}{2} \max_{0 \leqslant n \leqslant N} \|g_n\|_\infty + \max_{0 \leqslant n \leqslant N} \|w_n\|_\infty$$

which leads to (B.3). QED

APPENDIX C. PROOF OF THE CONVERGENCE TO THE ASYMPTOTIC STATE FOR FINITE MULTIBAKER CHAIN

In this appendix, we give the details of the proof of the asymptotic convergence to the stationary state for the finite multibaker chain discussed in Section 6.4.

C1. Inequality for the Second-order Derivative of the Cumulative Function $\partial_x^2 G_t$

We derive the inequality (6.12) for the second-order derivative of the cumulative function $\partial_x^2 G_t$. Since the forward time evolution (6.3a) and (6.6) keeps the smoothness of $G_t(n, x, y)$ with respect to x, we can derive the time evolution equation for the second-order derivative $\partial_x^2 G_t$ by differentiating (6.3a) and (6.6) with respect to x:

$$\partial_x^2 G_{t+1}(n, x, y) = \begin{cases} \frac{1}{4}\partial_{x'}^2 G_t(n+1, x', 2y)|_{x'=x/2}, & 0 \leqslant y < \frac{1}{2} \\ \frac{1}{4}\partial_{x'}^2 G_t(n+1, x', 1)|_{x'=x/2} & \\ \quad + \frac{1}{4}\partial_{x'}^2 G_t(n-1, x', 2y-1)|_{x'=(x+1)/2}, & \frac{1}{2} \leqslant y \leqslant 1 \end{cases} \tag{C.1}$$

where $n = 0, 1, 2, \ldots, N$ and $\partial_x^2 G_t(-1, x, y) = \partial_x^2 G_t(N+1, x, y) \equiv 0$. Equation (C.1) immediately gives the desired result (6.12):

$$\|\partial_x^2 G_t\| \leqslant \tfrac{1}{2}\|\partial_x^2 G_{t-1}\| \leqslant \cdots \leqslant (\tfrac{1}{2})^t \|\partial_x^2 G_0\| \tag{C.2}$$

where

$$\|\partial_x^2 G_t\| \equiv \max_{0 \leqslant n \leqslant N} \sup_{\substack{0 \leqslant x \leqslant 1 \\ 0 \leqslant y \leqslant 1}} |\partial_x^2 G_t(n, x, y)| \tag{C.3}$$

C2. Separation of the Cumulative Function into the x-Uniform Term and the Rest

Here, we show that the deviation δ_t of the cumulative function G_t from the x-uniform term $xG_t(n, 1, y)$, defined in (6.14b), obeys the inequality (6.14c). Indeed, the inequality (C.2) and the definition (6.14b) immediately give the desired estimation (6.14c) because

$$\begin{aligned} |\delta_t(n, x, y)| &\leqslant \|\partial_x^2 G_t\| \left\{ \frac{1}{x} \int_0^x dx' \int_0^{x'} dx'' + \int_0^1 dx' \int_0^{x'} dx'' \right\} \\ &\leqslant \frac{x+1}{2} \|\partial_x^2 G_t\| \leqslant \left(\frac{1}{2}\right)^t \|\partial_x^2 G_0\| \end{aligned} \tag{C.4}$$

C3. Noise Term in the Random Walk Equation (6.15a)

We give an explicit expression for the noise term η_t in the random walk equation (6.15a) and show that it obeys the inequality (6.15b). From

the time evolution equations (6.3a) and (6.6) with $x = y = 1$ and the definitions of the x-uniform term and the rest (6.14), we get (6.15a) together with the noise η_t:

$$\eta_t(n) = \tfrac{1}{2}[\delta_t(n+1, \tfrac{1}{2}, 1) - \delta_t(n-1, \tfrac{1}{2}, 1)] \qquad (0 \leqslant n \leqslant N) \tag{C.5}$$

where $\delta_t(-1, 1/2, 1) = \delta_t(N+1, 1/2, 1) = 0$. Then, as a result of (C.4), we have the desired result

$$|\eta_t(n)| \leqslant \tfrac{1}{2}\,|\delta_t(n+1, \tfrac{1}{2}, 1)| + \tfrac{1}{2}\,|\delta_t(n-1, \tfrac{1}{2}, 1)| \leqslant (\tfrac{1}{2})^t\, \|\partial_x^2 G_0\| \tag{C.6}$$

C4. Solution of the Random Walk Equation (6.15a)

Equation (6.15a) is solved with the aid of the discrete sine transformation, which is based on a formula valid for $m, m' = 1, 2, \ldots, N+1$:

$$\frac{2}{N+2} \sum_{n=1}^{N+1} \sin\left(\frac{\pi n}{N+2} m\right) \sin\left(\frac{\pi n}{N+2} m'\right) = \delta_{mm'} \tag{C.7}$$

To solve (6.15a), we set

$$h_t(n) \equiv G_t(n, 1, 1) - \left[\frac{\rho_+ - \rho_-}{N+2}(n+1) + \rho_-\right] \tag{C.8}$$

which satisfies the same equation as $G_t(n, 1, 1)$ with a different boundary condition:

$$h_{t+1}(n) = \tfrac{1}{2}[h_t(n-1) + h_t(n+1)] + \eta_t(n) \tag{C.9a}$$

$$h_t(-1) = h_t(N+1) = 0 \tag{C.9b}$$

By multiplying $\sin\{[(n+1)/(N+2)]\,\pi m\}$ to (C.9a) and summing over n from 0 to N, we obtain

$$\begin{aligned} \hat{h}_t(m) &= \cos\left(\frac{\pi m}{N+2}\right) \hat{h}_{t-1}(m) + \hat{\eta}_{t-1}(m) \\ &= \left(\cos\frac{\pi m}{N+2}\right)^t \hat{h}_0(m) + \sum_{s=1}^{t} \left(\cos\frac{\pi m}{N+2}\right)^{s-1} \hat{\eta}_{t-s}(m) \end{aligned} \tag{C.10}$$

where

$$\begin{aligned} \hat{h}_t(m) &\equiv \sum_{n=0}^{N} \sin\left(\frac{n+1}{N+2}\pi m\right) h_t(n) \\ \hat{\eta}_t(m) &\equiv \sum_{n=0}^{N} \sin\left(\frac{n+1}{N+2}\pi m\right) \eta_t(n) \end{aligned} \tag{C.11}$$

With the aid of the inversion formula (C.7), we obtain the desired solution for (C.9) and thus for (6.15a). Finally, the solution $h_t(n)$ is given by Eq. (6.16a).

C5. Asymptotic Behavior of the Solution of the Random Walk Equation (6.15a)

From (C.11) with $t=0$ and the upper bound (C.6) for η_t, we have

$$|\hat{h}_0(m)| \leqslant (N+1) \sup_{0 \leqslant n \leqslant N} |h_0(n)| \tag{C.12a}$$

$$|\hat{\eta}_t(m)| \leqslant (N+1)(\tfrac{1}{2})^t \, \|\partial_x^2 G_0\| \tag{C.12b}$$

On the other hand, for $1 \leqslant m \leqslant N+1$

$$\left|\cos \frac{\pi m}{N+2}\right| \leqslant \cos \frac{\pi}{N+2} \tag{C.13a}$$

and for $N>1$

$$\cos \frac{\pi}{N+2} > \frac{1}{2} \tag{C.13b}$$

Therefore, the solution (6.16a) of (6.15a) satisfies

$$\begin{aligned} |h_t(n)| &= \left| G_t(n, 1, 1) - \left[\frac{\rho_+ - \rho_-}{N+2}(n+1) + \rho_- \right] \right| \\ &\leqslant \frac{2(N+1)}{N+2} \sum_{m=1}^{N+1} \left\{ \left(\cos \frac{\pi}{N+2} \right)^t \sup_{0 \leqslant n \leqslant N} |h_0(n)| \right. \\ &\quad \left. + \|\partial_x^2 G_0\| \sum_{s=1}^{t} \left(\cos \frac{\pi}{N+2} \right)^{s-1} \left(\frac{1}{2} \right)^{t-s} \right\} \\ &\leqslant K \gamma_0^t \end{aligned} \tag{C.14}$$

where γ_0 is defined by Eq. (6.17b) and

$$K = \frac{2(N+1)^2}{N+2} \left[\sup_{0 \leqslant n \leqslant N} |h_0(n)| + \frac{2 \, \|\partial_x^2 G_0\|}{2 \cos[\pi/(N+2)] - 1} \right] \tag{C.15}$$

C6. Equation for $G_t(n, 1, y)$

As explained in Section 6, by substituting (6.14a) into (6.3a) and (6.6) and setting $x=1$, we obtain the equation of motion for $G_t(n, 1, y)$ which

is given by Eq. (6.18a) in terms of the transformation $\mathscr{T}_2$ defined by Eq. (6.18b) of Section 6. In these equations, the deviation $\delta G_t(n, 1, y)$ is given by

$$\delta G_t(n, 1, y) \equiv \begin{cases} \frac{1}{2}h_t(n+1), & \frac{1}{2} \leqslant y \leqslant 1, \quad 0 \leqslant n \leqslant N-1 \\ 0, & \text{otherwise} \end{cases} \tag{C.16}$$

and the "noise" ξ_t is

$$\xi_t(n, y) \equiv \begin{cases} \frac{1}{2}\delta_t(n+1, \frac{1}{2}, 2y), & 0 \leqslant y < \frac{1}{2} \\ \frac{1}{2}\delta_t(n+1, \frac{1}{2}, 1) - \frac{1}{2}\delta_t(n-1, \frac{1}{2}, 2y-1), & \frac{1}{2} \leqslant y \leqslant 1 \end{cases} \tag{C.17}$$

where $0 \leqslant n \leqslant N$ with conventions $\delta_t(-1, 1/2, y) = \delta_t(N+1, 1/2, y) \equiv 0$.

The inequalities (C.14) and (C.4) imply, respectively,

$$|\delta G_t(n, 1, y)| \leqslant \frac{K}{2}\gamma_0^t \tag{C.18}$$

$$|\xi_t(n, y)| \leqslant \left(\frac{1}{2}\right)^t \|\partial_x^2 G_0\| \tag{C.19}$$

so that the deviation and "noise" terms vanish exponentially.

APPENDIX D. FRACTAL DIMENSION OF THE STABLE MANIFOLDS OF THE REPELLER

In this appendix, we calculate the fractal dimension of the set Φ of phase points for which the escape time from a multibaker chain of length $N+1$ is infinite. This set is formed by the stable manifolds of the fractal repeller.

By definition, it is obvious that Φ is a set of phase points whose symbolic representations contain the symbols 0, 1,..., N in the right-hand side of their symbolic sequence:

$$\Phi = \sigma^{-1}\{\omega = \{\omega_j\}_{-\infty < j < \infty} \in \Omega: \omega_j \in \{0, 1, ..., N\} \ (j = 0, 1, ...)\} \tag{D.1}$$

where Ω is the space of all symbolic sequences generated by the multibaker map B and σ is the map inducing the symbolic representation (cf. Appendix A).

We calculate the Hausdorff dimension of the set $\Phi_k \equiv \Phi \cap \{[0, 1]^2\}_k$ ($k = 0, 1, ..., N$). First, we introduce auxiliary sets and study their properties. Let $\bar{\omega} = \{\omega_j\}_{0 \leqslant j \leqslant m}$ be a finite symbolic sequence of length $m+1$, which

consists of symbols 0, 1, 2,..., N and satisfies $\omega_0 = k$ and $\omega_{j+1} = \omega_j \pm 1$, and $\Sigma_{\bar{\omega}}^{(k,m)}$ be the corresponding cylindrical set:

$$\Sigma_{\bar{\omega}}^{(k,m)} \equiv \{\omega' = \{\omega'_j\}_{-\infty < j < \infty} \in \Omega: \omega'_0 = k, \omega'_j = \omega_j \ (j = 1,..., m)\} \quad \text{(D.2)}$$

Further we denote the union of these cylindrical sets corresponding to fixed k and m as $\Sigma_{(k,m)}$:

$$\Sigma_{(k,m)} \equiv \bigcup_{\bar{\omega}}{}' \Sigma_{\bar{\omega}}^{(k,m)} \quad \text{(D.3)}$$

Obviously, we have

$$\sigma^{-1}\Sigma_{(k,m)} \supset \sigma^{-1}\Sigma_{(k,m')} \qquad (m' \geqslant m) \quad \text{(D.4a)}$$

$$\Phi_k = \bigcap_{m=0}^{\infty} \sigma^{-1}\Sigma_{(k,m)} \quad \text{(D.4b)}$$

The number of cylindrical sets $\sigma^{-1}\Sigma_{\bar{\omega}}^{(k,m)}$ can be counted as follows. Let us introduce an $(N+1)\times(N+1)$ matrix $A = \{A_{ij}\}$ $(0 \leqslant i, j \leqslant N)$:

$$A_{ij} = \begin{cases} 1, & i = j \pm 1 \\ 0, & \text{otherwise} \end{cases} \quad \text{(D.5)}$$

Then for a finite symbolic sequence $\bar{\omega} = \{\omega_j\}_{0 \leqslant j \leqslant m}$, we have

$$A_{\omega_0\omega_1} A_{\omega_1\omega_2} \cdots A_{\omega_{m-1}\omega_m} = \begin{cases} 1 & \text{if the cylindrical set } \sigma^{-1}\Sigma_{\bar{\omega}}^{(k,m)} \text{ exists} \\ 0 & \text{otherwise} \end{cases} \quad \text{(D.6)}$$

which leads to

$$\begin{aligned} &\{\text{number of cylindrical sets } \sigma^{-1}\Sigma_{\bar{\omega}}^{(k,m)}\} \\ &\quad \equiv N_m = \sum_{\omega_1=0}^{N} \cdots \sum_{\omega_m=0}^{N} A_{\omega_0\omega_1} A_{\omega_1\omega_2} \cdots A_{\omega_{m-1}\omega_m} \\ &\quad = \sum_{n=0}^{N} (A^m)_{kn} = \frac{2}{N+2} \sum_{\substack{s=1 \\ s:\ \text{odd}}}^{N+1} \left(2\cos\frac{\pi s}{N+2}\right)^m \\ &\qquad \times \sin\left(\frac{k+1}{N+2}\pi s\right) \cot\left(\frac{\pi s}{2(N+2)}\right) \end{aligned} \quad \text{(D.7)}$$

The equality (D.7) can be shown straightforwardly by diagonalizing the matrix $A = \{A_{ij}\}$ in terms of a discrete sine transformation discussed in Section C4 of Appendix C.

On the other hand, as shown in Appendix A, each cylindrical set $\sigma^{-1}\Sigma_{\bar{\omega}}^{(k,m)}$ has the structure of [cf. (1) of Lemma A]

$$\sigma^{-1}\Sigma_{\bar{\omega}}^{(k,m)} = \{[a_m, b_m] \times [0, 1]\}_k \tag{D.8}$$

where $b_m - a_m = 1/2^m$, and two cylindrical sets $\sigma^{-1}\Sigma_{\bar{\omega}}^{(k,m)}$ and $\sigma^{-1}\Sigma_{\bar{\omega}'}^{(k,m)}$ corresponding to different finite sequences $\bar{\omega}$ and $\bar{\omega}'$ are disjoint [cf. (A.16) for the set $\sigma^{-1}\Sigma_{\bar{\omega}}^{(k,m)} \equiv \bigcap_{j=0}^{m} B^{-j}\{[0, 1]^2\}_{\omega_j}$]

$$\sigma^{-1}\Sigma_{\bar{\omega}}^{(k,m)} \cap \sigma^{-1}\Sigma_{\bar{\omega}'}^{(k,m)} = \varnothing \tag{D.9}$$

Now, we calculate the Hausdorff dimension of the set Φ_k. Let us consider a covering of Φ_k which consists of $1/2^m \times 1/2^m$ squares. Because of (D.4), the minimum number of such squares necessary for covering Φ_k can be estimated as the minimum number v_m of squares necesary for covering the set $\sigma^{-1}\Sigma_{(k,m)}$. Since the number of squares necessary for covering each cylindrical set $\sigma^{-1}\Sigma_{\bar{\omega}}^{(k,m)}$ is equal to 2^m [cf. (D.8)] and different cylindrical sets are disjoint [cf. (D.9)], the number v_m is equal to the product of 2^m and the number N_m of cylindrical sets $\sigma^{-1}\Sigma_{\bar{\omega}}^{(k,m)}$: $v_m = 2^m N_m$. Thus, the D-dimensional measure of the set Φ_k is estimated as the $m \to +\infty$ limit of

$$\begin{aligned} l_m^D v_m &= \left(\frac{1}{2^m}\right)^D 2^m N_m \\ &= \frac{2}{N+2} \sum_{\substack{s=1 \\ s:\ \text{odd}}}^{N+1} \left(2^{2-D} \cos\frac{\pi s}{N+2}\right)^m \\ &\quad \times \sin\left(\frac{k+1}{N+2}\pi s\right) \cot\left[\frac{\pi s}{2(N+2)}\right] \end{aligned} \tag{D.10}$$

where $l_m = 1/2^m$ is the length of the side of each covering square. For $m \to +\infty$, the expression (D.10) diverges if $2^{2-D}\cos[\pi/(N+2)] > 1$ and vanishes if $2^{2-D}\cos[\pi/(N+2)] < 1$. Hence the Hausdorff dimension D_H of the set Φ_k is determined from $2^{2-D_H}\cos[\pi/(N+2)] = 1$, or

$$D_H = 2 + \frac{\ln\cos[\pi/(N+2)]}{\ln 2} \tag{D.11}$$

Moreover, the corresponding Hausdorff measure of Φ_k is estimated as

$$\mu_H(\Phi_k) \simeq \liminf_{m\to\infty} l_m^{D_H} v_m = \frac{2Q_N}{N+2} \sin\left(\frac{k+1}{N+2}\pi\right) \tag{D.12a}$$

where the prefactor is given by

$$Q_N = \begin{cases} \cot\left[\dfrac{\pi}{2(N+2)}\right], & \text{for } N \text{ odd} \\ \cot\left[\dfrac{\pi}{2(N+2)}\right] - \tan\left[\dfrac{\pi}{2(N+2)}\right], & \text{for } N \text{ even} \end{cases} \tag{D.12b}$$

As D_H is independent of the site coordinate k, the Hausdorff dimension of the stable manifolds Φ of the repeller is equal to D_H. On the contrary, as seen in (D.12), the D_H-dimensional measure of $\Phi_k = \Phi \cap \{[0, 1]^2\}_k$ depends sinusoidally on the site coordinate k: $\mu_H(\Phi_k) \sim \sin[\pi(k+1)/(N+2)]$.

ACKNOWLEDGMENTS

The authors thank Prof. K. Fukui and Prof. M. Yamaguti for their continuous interest, encouragement, and valuable comments. S. T. is grateful to Prof. I. Prigogine, Dr. I. Antoniou, and Dr. Z. Suchanecki, as many ideas of the present work are deeply indebted to his collaboration with them in Brussels. P. G. thanks the National Fund for Scientific Research (FNRS Belgium) for financial support. The work is partly supported by a Grant-in-Aid for Scientific Research and a grant under the International Scientific Research Program both from the Ministry of Education, Science and Culture of Japan as well as by the Communauté Française de Belgique under ARC contract 93/98-166.

REFERENCES

1. J. Lebowitz and H. Spohn, *J. Stat. Phys.* **19**:633 (1978); H. Spohn, *Rev. Mod. Phys.* **53**:569 (1980); L. A. Bunimovich and Y. G. Sinai, *Commun. Math. Phys.* **78**:479 (1980).
2. S. Grossman and H. Fujisaka, *Phys. Rev. A* **26**:1779 (1982).
3. S. Thomae, Chaos-induced diffusion, in *Statics and Dynamics of Nonlinear Systems*, G. Benedek *et al.*, eds. (Springer, Berlin, 1983), pp. 204–210.
4. P. Gaspard, *Phys. Lett. A* **168**:13 (1992).
5. H. H. Hasegawa and D. J. Driebe, *Phys. Lett. A* **168**:18 (1992).
6. P. Gaspard, *J. Stat. Phys.* **68**:673 (1992).
7. P. Gaspard, *Chaos* **3**:427 (1993).
8. H. H. Hasegawa and D. J. Driebe, *Phys. Rev. E* **50**:1781 (1994).
9. S. Tasaki, A. Hakmi, and I. Antoniou, To appear (1994).
10. M. Pollicott, *Invent. Math.* **81**:413 (1985); **85**:147 (1986).
11. D. Ruelle, *Phys. Rev. Lett.* **56**:405 (1986); *J. Stat. Phys.* **44**:281 (1986).
12. P. Gaspard and S. Tasaki, To appear.
13. I. Prigogine, *Non-equilibrium Statistical Mechanics* (Wiley, New York, 1962).

14. I. Prigogine, C. George, F. Henin, and L. Rosenfeld, *Chem. Scripta* **4**:5–32 (1973); R. Balescu, *Equilibrium and Nonequilibrium Statistical Mechanics* (Wiley, New York, 1975); T. Petrosky and I. Prigogine, *Physica A* **175**:146–209 (1991); *Proc. Natl. Acad. Sci. USA* **90**:9393 (1993); I. Antoniou and I. Prigogine, *Physica A* **192**:443–464 (1993).
15. J.-P. Eckmann and D. Ruelle, *Rev. Mod. Phys.* **57**:617 (1985).
16. D. Ruelle, *Chaotic Evolution and Strange Attractors* (Cambridge University Press, Cambridge, 1989).
17. S. Tasaki and P. Gaspard, In *Towards the Harnessing of Chaos*, M. Yamaguti, ed. (Elsevier, Amsterdam, 1994), pp. 273–288.
18. R. C. Toleman, *The Principles of Statistical Mechanics* (Oxford University Press, Oxford, 1938; reprinted Dover, New York, 1979).
19. G. deRham, *Rend. Sem. Mat. Torino* **16**:101 (1957).
20. M. Hata and M. Yamaguti, *Jpn. J. Appl. Math.* **1**:183 (1984).
21. M. Hata, In *Patterns and Waves*, T. Nishida, M. Mimura, and H. Fujii, eds. (Kinokuniya, Tokyo, and North-Holland, Amsterdam, 1986), pp. 259–278.
22. S. Tasaki, I. Antoniou, and Z. Suchanecki, *Phys. Lett. A* **179**:97 (1993).
23. E. Hewitt and K. Stromberg, *Real and Abstract Analysis* (Springer-Verlag, New York, 1975).
24. P. Billingsley, *Ergodic Theory and Information* (Wiley, New York, 1965).
25. T. Takagi, *Proc. Phys. Math. Soc. Japan Ser. II* **1**:176 (1903).
26. D. Ornstein, *Science* **243**:182 (1989).
27. I. P. Cornfeld and Ya. G. Sinai, In *Dynamical Systems II* (Springer-Verlag, Berlin, 1989).
28. Y. Oono and Y. Takahashi, *Prog. Theor. Phys.* **63**:1804 (1980); Y. Takahashi and Y. Oono, *Prog. Theor. Phys.* **71**:851 (1984).
29. S. Tasaki, Z. Suchanecki, and I. Antoniou, *Phys. Lett. A* **179**:103 (1993).
30. T. Tél and E. Ott, eds., Chaotic Scattering, *Chaos* **3**(4):417–706 (1993).